LBL-28718
Preprint

Center for Advanced Materials

CAM

Submitted to Physical Review Letters B

On the Phase Diagram of the Superconducting Oxide $YBa_2Cu_3O_{6+\delta}$

A.G. Khachaturyan, S.V. Semonovskaya, and J.W. Morris, Jr.

March 1990

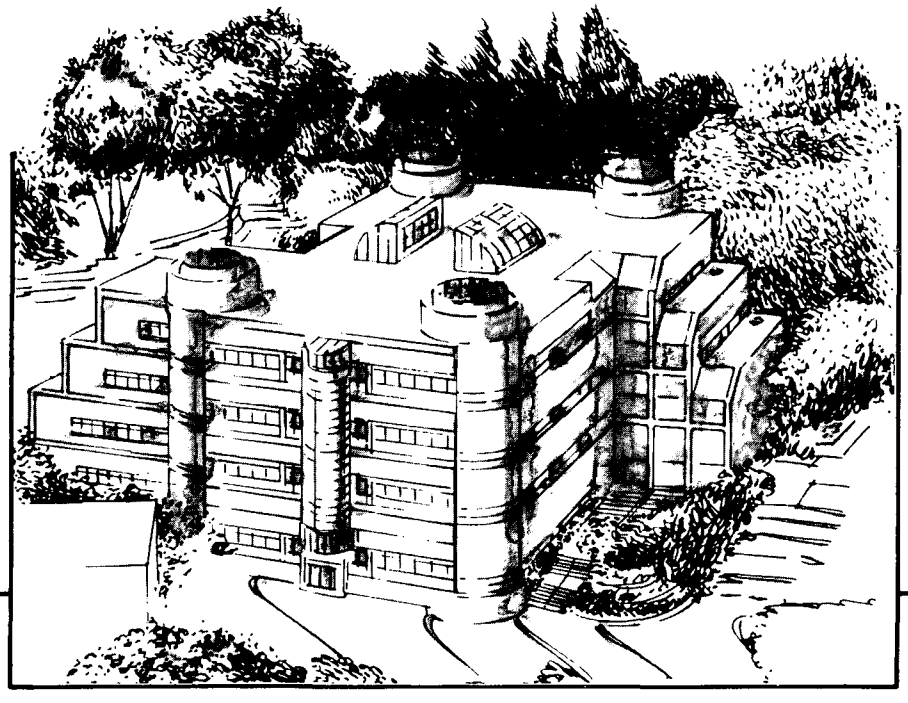

Materials and Chemical Sciences Division

Lawrence Berkeley Laboratory • University of California

ONE CYCLOTRON ROAD, BERKELEY, CA 94720 • (415) 486-4755

Prepared for the U.S. Department of Energy under Contract DE-AC03-76SF00098

LOAN COPY
Circulates
For 2 weeks
Bldg. 50 Library.
Copy 2
LBL-28718

DISCLAIMER

This document was prepared as an account of work sponsored by the United States Government. While this document is believed to contain correct information, neither the United States Government nor any agency thereof, nor the Regents of the University of California, nor any of their employees, makes any warranty, express or implied, or assumes any legal responsibility for the accuracy, completeness, or usefulness of any information, apparatus, product, or process disclosed, or represents that its use would not infringe privately owned rights. Reference herein to any specific commercial product, process, or service by its trade name, trademark, manufacturer, or otherwise, does not necessarily constitute or imply its endorsement, recommendation, or favoring by the United States Government or any agency thereof, or the Regents of the University of California. The views and opinions of authors expressed herein do not necessarily state or reflect those of the United States Government or any agency thereof or the Regents of the University of California.

LBL 28718

On the Phase Diagram of the Superconducting Oxide $YBa_2Cu_3O_{6+\delta}$

A. G. Khachaturyan*, S. V. Semonovskaya,* J. W. Morris, Jr†

†Center for Advanced Materials
Materials and Chemical Sciences Division
Lawrence Berkeley Laboratory
1 Cyclotron Road
Berkeley, CA 94720
and
Department of Materials Science and Mineral Engineering
University of California
and
*Department of Mechanics and Materials Science
Rutgers University, Piscataway, NJ

March 1990

This work was supported by the Director, Office of Energy Research, Office of Basic Energy Science, Materials Sciences Division of the U. S. Department of Energy under Contract No. *DE-AC03-76SF00098* (JWM) and the National Science Foundation under grant No. *NSF-DMF-88-17922* (AGK)

On the Phase Diagram of the Superconducting Oxide $YBa_2Cu_3O_{6+\delta}$

A.G. Khachaturyan*, S.V. Semenovskaya*, J.W. Morris, Jr.†

*Department of Mechanics and Materials Science, Rutgers University, P.O. Box 909, Piscataway, NJ 08855
†Center for Advanced Materials, Lawrence Berkeley Laboratory, and Department of Materials Science and Engineering, University of California, Berkeley, CA 94720

Abstract

Recent research suggests that the high-temperature superconducting oxide, $YBa_2Cu_3O_{6+\delta}$, assumes three equilibrium phases as the oxygen content (δ) is varied at low temperature: a tetragonal phase (T) that is stoichiometric at $\delta = 0$, an orthorhombic phase (O) at $\delta = 1$, and an intermediate orthorhombic phase (O') that is stoichiometric at $\delta = 0.5$. The O' phase is characterized by a secondary ordering of oxygen in the basal plane of the O phase by the concentration wave $\mathbf{k}_1 = \frac{2\pi}{a}(\frac{1}{2}00)$. We compute a phase diagram and a congruent transformation for the system on the assumption that the oxygen-oxygen interaction on the basal sublattice is a screened coulomb potential supplemented by a short-range attractive potential, which is necessary to stabilize the O' phase against a competing ordered phase (the "2a x 2a" phase). The potential is fit to experimental temperatures for the direct transition T⇌O and O⇌O' at $\delta = 0.5$. The model predicts a narrow O' equilibrium field at low temperature capped by a peritectic reaction to a mixture of T and O phases, predicts that the O' phase appears over a broad composition range on quenching, and yields phase transformation behavior in good agreement with experiment.

I Introduction.

Shortly after the discovery of the high-temperature superconducting oxide $YBa_2Cu_3O_{6+\delta}$ it was recognized that the oxide appeared in at least two crystal structures: a tetragonal structure with the stoichiometric composition $YBa_2Cu_3O_6$ (T-phase) and an orthorhombic structure with the stoichiometric composition $YBa_2Cu_3O_7$ (O-phase) in which the additional oxygen atoms are ordered in the basal (Cu-O) plane of the three-layer perovskite cell. Given the existence of two distinct structures and the possibility of converting them into one another by changing the oxygen content, it necessarily follows that non-stoichiometric samples with intermediate values of the oxygen content (δ) are unstable with respect to two-phase decomposition at sufficiently low temperature [1]. If one assumes that only the T and O phases appear in equilibrium then it is possible to sketch the possible forms of the phase diagram [1]. The present authors [2] calculated a phase diagram for the equilibrium of the T and O phases, using a crystal lattice gas model with a long-range pairwise oxygen-oxygen interaction, and fitting this model to the available data for the T→O ordering temperature. More recent experimental studies [3-11] have documented the low-temperature decomposition of $YBa_2Cu_3O_{6+\delta}$ and the coexistence of the T

and O phases. However, the experimental data also suggest that at least one other equilibrium phase appears as the oxygen concentration (δ) is varied.

The low-temperature decomposition of $YBa_2Cu_3O_{6+\delta}$ was confirmed in a number of investigations by electron microscopic [3-8], x-ray [9-11], and Raman spectroscopic [12] methods. Sarikaya and Stern [3] and by Hiroi et. al. [6] found direct evidence for the coexistence of the tetragonal (T) and orthorhombic (O) phases at low temperature through high resolution electron microscopy. Sood et. al. [10] reported qualitative agreement with the phase diagram predicted in ref. [2] on the basis of infrared absorption and X-ray diffraction data.

Detailed study of the system showed that the decomposition reaction is complicated by the appearance of other ordered structures that involve different distributions of oxygen atoms over the basal planes of the unit cell. For example, You et al.[9] observed splitting in the x-ray diffraction pattern of the O-phase which they interpreted as a coexistence of two orthorhombic phases with stoichiometries close to 7 and to 6.7. Van Tandeloo et al. [13], Chen et al. [4] , Werder et al. [5], Fleming et al. [14] found intermediate ordered structures and characterized them. It seems clear that most of these observations concern metastable structures that form on cooling non-stoichiometric material. The intermediate ordered states typically appear in the form of short-range ordered regions with coherency length in the range of 10 - 20 Å; several have periodicities that can be anticipated on the basis of the well-known Magneli series of intermediate ordered structures in non-stoichiometric oxides [15].

However, it has been suspected for some time that the ordered structure that is obtained by doubling the repeat period of oxygen in the basal plane may be an equilibrium phase (the O' phase). This structure has the stoichiometric formula $YBa_2Cu_3O_{6.5}$. It is obtained from the O-phase by a secondary ordering on the basal sublattice of oxygen sites generated by a plane concentration wave with the wave vector $\mathbf{k_1} = \frac{2\pi}{a}(\frac{1}{2}00)$, and hence produces a diffraction maximum at the position $(\frac{1}{2}00)$. While early studies found only short-range order of the $(\frac{1}{2}00)$ type, suggesting that the phase is not stable, recent high-resolution electron microscopic studies by Amelinckx et al. [16], Reyes-Gasga et al. [17] and by Beyers et al.[18] have documented the presence of $(\frac{1}{2}00)$ double-period ordered phase domains with size as large as several hundred Å. While it still remains possible that the observed O' domains are metastable products of the ordering of non-stoichiometric material, the balance of the evidence suggests that the O' structure is an equilibrium phase. It is, therefore, useful to investigate possible forms of the phase diagram that include a stable O' phase.

The experimental data of Reyes-Gasga et al. [17] and Beyers et al.[18] also sheds some light on the shape of the O' phase field and its relation to the T and O phases. They only found sizeable domains of the O' structure for oxygen concentrations if the composition almost precisely equal to the stoichiometric value, 6.5, which suggests that the equilibrium phase field is extremely narrow. However, microdomains of the O' phase were observed over a broad concentration range above $\delta = 0.5$. These observations suggest the existence of a two-phase O' + O field of the phase diagram where precipitates of the inter-

mediate O' phase coarsen very slowly because of the slow diffusion kinetics. In other relevant experiments, Amelinckx et al.[16] and Reyes-Gasga et al. [17] observed the disappearance of $(\frac{1}{2}00)$-type diffraction maxima when $YBa_2Cu_3O_7$ was isothermally reduced in the electron microscope at temperatures well below the second-order transition temperature, T_0, between the disordered T phase and the orthorhombic O phase at $\delta=0.5$ ($T_0 \approx$ 700°C[19]). This suggests that the O' phase is formed from the orthorhombic O-structure rather than directly from the disordered tetragonal phase.

The only theoretical effort known to us that attempts to construct a phase diagram for the system that includes the O' is that by deFontaine, et al. [20]. They used a two-dimensional model that considered only the oxygen atoms in the basal plane, assumed an oxygen-oxygen interaction that is confined to near neighbors, and adjusted the relative magnitudes of the near-neighbor interactions to stabilize the two-dimensional analogue of the O' structure. The approach is suspect since virtually all successful analyses of bonding in oxides [21-24] assume an O-O interaction that is largely coulombic and, hence, long-range; the long-range interaction in $YBa_2Cu_3O_{6+\delta}$ is indicated by the registry of oxygen atoms in successive basal planes of the three-layer perovskite unit cell, which is an essential element of the ordered structures. Moreover, the cluster-variation method used in the calculation converges poorly at low temperature, so the calculated diagram is inaccurate there (in the published diagram [20] the low-temperature phase fields, which are in many respects the most interesting part of the diagram, were simply guessed).

These problems are avoided in the concentration-wave method that was used to calculate the diagram in ref. [2], which does not impose any constraint on the range of an effective oxygen-oxygen interaction and converges easily at low temperature. This method is also approximate, since it is necessary to use the mean-field approximation to produce a mathematically tractable model when the interaction extends beyond the immediate neighbors. However, while mean-field methods are inaccurate for systems with near-neighbor bonding, they become increasingly accurate as the range of the interatomic interaction grows larger [25], and are exact in the limit of low temperature or high order [26]. They should, hence, be useful in analyzing the low-temperature phase relationships among the ordered structures of $YBa_2Cu_3O_{6+\delta}$.

In the following we calculate a phase diagram for $YBa_2Cu_3O_{6+\delta}$ as a function of the oxygen concentration parameter, δ, on the assumption that the three phases, T, O and O' are possible equilibrium structures. Since these phases only differ through reconfigurations of oxygen atoms on the basal sublattice of oxygen sites in the three-layer perovskite structure of $YBa_2Cu_3O_{6+\delta}$, the relative energies of the phases are governed by the effective interaction of the oxygen atoms. We first assume that the effective O-O interaction is a coulomb potential that is screened by free charge carriers. However, with this potential the O' phase is metastable (though it would appear on cooling) and is less stable than an alternative ordered structure with a $(\frac{11}{22}0)$ pattern. Both these effects disappear if small, short-range corrections to the coulomb potential are taken into consideration; in fact, a short-range perturbation is almost certainly present for physical reasons.

The phase diagram produced by a screened coulomb potential with a short-range perturbation can be computed by fitting to two experimental observations: The T⇌O and O⇌O' transformation temperatures at $\delta = 0.5$. Both the equilibrium phase diagram and the congruent transformation diagram can then be calculated. The resulting potential provides a reasonable value for the dielectric constant of the oxide, which provides an internal check on its physical consistency. The equilibrium diagram is consistent with experimental evidence in several respects: it includes both the O and O' phases, it provides a narrow equilibrium field for the O' phase in agreement with the results of Amelinckx et al. [16], Reyes-Gasga et al. [17], and Beyers et al. [18], it predicts a peritectoid reaction, O' → T+O, at the top of the O' field in agreement with the x-ray data of Sood et al. [10], and it yields equilibrium concentrations of the coexisting T and O phases at 200°C that agree with the observations of Sood et al. [10] and Radhakrishnan et al. [11]. The associated congruent transformation diagram suggests that the O' phase can form through a congruent secondary ordering reaction of the O-phase on cooling over a broad range of oxygen contents.

II. The Free Energy

The energy of a particular configuration of atoms over an excess set of lattice sites is given by the Hamiltonian

$$H = \frac{1}{2}\sum_{\mathbf{rr'}} W(\mathbf{r}-\mathbf{r'})c(\mathbf{r})c(\mathbf{r'}) \tag{1}$$

where $W(\mathbf{r}-\mathbf{r'})$ is the two-body interaction and $c(\mathbf{r})$ specifies the configuration; it has the value 1 at occupied lattice sites and the value 0 elsewhere. Given that the bonding function, $W(\mathbf{r})$, is long-range, it is necessary to invoke the mean-field approximation to evaluate the free energy from this Hamiltonian. There is no available analytical technique to treat the correlation effects for a long-range interaction; all known techniques become intractable when the interaction is significant beyond the immediate neighbor shells.

On the positive side, the accuracy of the mean-field approximation increases with the range of interaction. Its quantitative accuracy was assessed by Vaks et al. [25] who provide an estimate for the temperature range, ΔT, around the second-order transition temperature, T_o, in which the mean-field approximation fails:

$$\frac{\Delta T}{T_o} \sim \frac{1}{N^2} \tag{2}$$

where N is a number of crystal lattice cells inside a sphere of interaction whose radius, r_o, is determined by the equation

$$r_0^2 = \frac{\sum_{\mathbf{r}} r^2 W(r)}{\sum_{\mathbf{r}} W(r)} \tag{3}$$

The interaction radius in $YBa_2Cu_3O_{6+\delta}$ must at least satisfy the inequality $r_0 > 3a$, where a is the lattice parameter of the parent perovskite cell. Hence $N \approx 20$, and $\Delta T/T_0$ is in the range 10^{-2}-10^{-3}. Since $T_0 \approx 1000$ K for the ordering reactions of interest to us, ΔT is in the range 1-10 K. Even if this estimate is too optimistic, it suggests that the mean-field approximation is a reasonable one unless the temperature is very close to a second-order transition temperature. Moreover, the accuracy of the mean-field approximation improves with decreasing temperature; it is asymptotically correct at low temperature irrespective of the interaction radius [26]. Since we are mainly interested in the low temperature behavior of the system the mean-field approximation should be adequate for our purposes.

Applying the mean-field approximation yields the configurational energy

$$E = \frac{1}{2} \sum_{\mathbf{rr'}} W(\mathbf{r}-\mathbf{r'}) n(\mathbf{r}) n(\mathbf{r'}) \tag{4}$$

where $n(\mathbf{r})$ is the probability that an atom occupies the site at position, $\mathbf{r}$, on the basal sublattice of oxygen sites. Using the Fourier transform to represent the occupation probability function, $n(\mathbf{r})$, as a superposition of concentration waves,

$$n(\mathbf{r}) = \sum_{\mathbf{k}} \tilde{n}(\mathbf{k}) e^{-i\mathbf{kr}} \tag{5}$$

where $\mathbf{k}$ is an admissible wave vector and $\tilde{n}(\mathbf{k})$ is the amplitude of the $\mathbf{k}^{th}$ concentration wave within the first Brillouin zone, the energy can be rewritten

$$E = \frac{1}{2N} \sum_{\mathbf{k}} V(\mathbf{k}) |\tilde{n}(\mathbf{k})|^2 \tag{6}$$

where N is the number of sites on the basal sublattice and $V(\mathbf{k})$ is the Fourier transform of the interaction potential, $W(\mathbf{r})$:

$$V(\mathbf{k}) = \sum_{\mathbf{r}} W(\mathbf{r}) e^{-i\mathbf{kr}} \tag{7}$$

The factor $|\tilde{n}(\mathbf{k})|^2$ is the squared amplitude of a concentration wave of wave vector **k**, which is a plane wave in three-dimensional space. The Helmholtz free energy is obtained from equation (6) by adding the mean-field value of the configurational entropy:

$$S = -k_B \sum_{\mathbf{r}} \{n(\mathbf{r})\ln[n(\mathbf{r})] + [1-n(\mathbf{r})]\ln[1-n(\mathbf{r})]\} \tag{8}$$

Hence the free energy of the system characterized by the temperature, volume, and oxygen distribution, n(**r**), can be written

$$F(T,\{n(\mathbf{r})\}) = \frac{1}{2N}\sum_{\mathbf{k}} V(\mathbf{k})|\tilde{n}(\mathbf{k})|^2 + k_B T\sum_{\mathbf{r}} \{n(\mathbf{r})\ln[n(\mathbf{r})] + [1-n(\mathbf{r})]\ln[1-n(\mathbf{r})]\} \tag{9}$$

III The Concentration-Wave Method

Given the long range of the oxygen-oxygen interaction in $YBa_2Cu_3O_{6+\delta}$ we use the concentration wave method [27-29] to analyze the structures and thermodynamic behavior of the stable ordered phases. This method allows us to predict the atomic structures of stable phases formed by ordering or decomposition of a high-temperature disordered phase if the effective interatomic interaction, W(**r**), is known. The concentration wave method has the important property that it does not impose any limitation on the interaction radius, which is especially important in the study of ceramic materials where the interaction is inherently long-range. Other analytical techniques, such as the "cluster-variation method", become intractable when the interaction extends beyond the immediate neighbors.

The concentration-wave method identifies the stable ordered structures in a simple sequence that can be illustrated by considering the ordering behavior of an oxide like $YBa_2Cu_3O_{6+\delta}$ as it is cooled. At sufficiently high temperatures the free energy function (eq. (9)) is dominated by the entropy term. The free energy is minimized when the oxygen atoms are randomly distributed over the available sites, in which case,

$$n(\mathbf{r}) = c \tag{10}$$

where c is the fraction of interstitial sites on the basal sublattice occupied by oxygen atoms. The value c is related to the stoichiometry parameter, δ, in the chemical formula $YBa_2Cu_3O_{6+\delta}$ by

$$c = \frac{\delta}{2} \tag{11}$$

The host atoms, Y, Ba, Cu, and O, form a fixed background frame that has tetragonal symmetry. Hence the crystal symmetry of $YBa_2Cu_3O_{6+\delta}$ is tetragonal when the oxygen

atoms in the basal plane are disordered. The corresponding phase will be called the T phase.

At low temperature the disordered phase always looses its stability with respect to a spatial heterogeneity which is described by the soft concentration waves. The amplitudes of the soft concentration waves are the long-range order parameters. In the mean field approximation the soft concentration waves are those whose wave vectors, **k**, minimize V(**k**)[27-29]. If the minimum of V(**k**) falls at $\mathbf{k}_o$, these wave vectors are the members of the star of $\mathbf{k}_o$, $\{\mathbf{k}_o^j\}$, the set of all wave vectors, $\mathbf{k}_o^j$, in the first Brillouin zone that can be obtained from $\mathbf{k}_o$ by symmetry operations of the symmetry group of the disordered phase. By symmetry,

$$V(\mathbf{k}_o) = V(\mathbf{k}_o^j) = \min V(\mathbf{k}) \tag{12}$$

The occupation probabilities, n(**r**), in the most stable ordered phase that is formed on cooling are generated by the soft concentration waves, and are described by the equation

$$n(\mathbf{r}) = c + c\eta \sum_j \gamma_j \exp(i\mathbf{k}_o^j \mathbf{r}) \tag{13}$$

where the γ_j are constants whose values are determined by symmetry only and η is a long range order (lro) parameter.

There are two kinds of minima for an arbitrary function, V(**k**), with the symmetry of the disordered lattice [27, 30]: symmetry minima and accidental minima. At a symmetry minimum the necessary condition, $\delta V(\mathbf{k})/\delta\mathbf{k} = 0$ at $\mathbf{k} = \mathbf{k}_o$, is automatically satisfied because of the symmetry of the reciprocal lattice point $\mathbf{k}_o$. Such high symmetry points are the Lifshitz points in **k**-space, and are characteristic of the geometry of the disordered phase crystal lattice . The accidental minima where $\delta V(\mathbf{k})/\delta\mathbf{k} = 0$ are associated with the specific mathematical form of the interaction potential, W(**r**). They occupy positions in **k**-space that shift with infinitesimal variations of the potential, W(**r**). Accidental minima may or may not be present.

For the interstitial sublattice shown in Fig.1 all Lifshitz points fall at mid-points of the reciprocal lattice vectors of the sublattice. The interaction potentials, W(**r**), that are of interest in this work are repulsive and monotonically decreasing. In can be shown in general that such potentials produce a minimum in V(**k**) at the point $\mathbf{k}_o = \frac{2\pi}{a}(100)$, which is due to the Lifshitz point at the mid-point of the interstitial lattice reciprocal lattice vector (200). The star of this vector contains only the vector itself. The atom distribution of the ordered phase generated by this wave vector is, by equation (14),

$$n(\mathbf{r}) = c + c\eta_o \exp(i\mathbf{k}_o\mathbf{r}) = c + c\eta_o \cos(\mathbf{k}_o\mathbf{r}) \tag{15}$$

where the coefficient γ is chosen to be equal to 1 to provide the conventional definition of lro parameter η within the range between 0 and 1.

Since the vector $\mathbf{k}_o$ is one-half of a reciprocal lattice vector in k-space, then $\cos(\mathbf{k}_o\mathbf{r})$ takes only two values, ± 1, at lattice sites, and $n(\mathbf{r})$ has one of the two values $n_\pm = c \pm c\eta_o$. By the definition of the completely ordered state the occupation probability, $n(\mathbf{r})$, should have the value one if the site is occupied and the value zero if it is vacant. Given equation (15) these conditions show that the fully ordered state determined by the wave vector $\mathbf{k}_0$ has the stoichiometric composition $c = c_{st} = \frac{1}{2}$ and the maximum long range order parameter $\eta = 1$.

If the composition of a primary ordered phase deviates from its exact stoichiometry, disorder is inevitable and the entropy cannot fall to zero at 0 K. Such a situation violates the third law of thermodynamics. To comply with the third law a non-stoichiometric ordered phase must transform in one of two ways as the temperature decreases: it must undergo secondary ordering into a stoichiometric ordered phase or it must decompose into a mixture of stoichiometric phases. The equilibrium transformation minimizes the free energy. However, the transformation that actually occurs is also influenced by the relative kinetics of all reactions that lower the free energy. Secondary ordering reactions may occur congruently even if equilibrium requires decomposition if the kinetics of decomposition are relatively slow. The theory of the secondary ordering [28,29] shows that the type of the secondary reaction (and the superlattice wave vector of the concentration waves generating the secondary transformation) is determined by the minima of the function:

$$\tilde{V}(\mathbf{k}) = \frac{V(\mathbf{k}) + V(\mathbf{k} - \mathbf{k}_o)}{2} \tag{16}$$

if the primary ordered phase is described by the distribution (15). The possible secondary ordered phases are fixed by the minima of $\tilde{V}(\mathbf{k})$; the preferred secondary ordering vector is fixed by the least minimum of $\tilde{V}(\mathbf{k})$.

If the least minimum of $\tilde{V}(\mathbf{k})$ falls at $\mathbf{k} = 0$ then isostructural decomposition is preferred and the system has a stable or metastable miscibility gap between two primary ordered phases with different stoichiometries. If the least minimum of $\tilde{V}(\mathbf{k})$ falls at the finite vector, $\mathbf{k}_1$, then the preferential reaction is a secondary ordering into a structure that is determined by the members of the star $\{\mathbf{k}_1^j\}$ of $\mathbf{k}_1$. The ordered phase is generated by superposing concentration waves with the superlattice wave vectors $\{\mathbf{k}_1^j\}$ on the dominant concentration wave that generates the primary ordered structure. The atomic distribution in the secondary ordered phase is :

$$n_1(\mathbf{r}) = c + c\eta_o \cos(\mathbf{k}_o\mathbf{r}) + c\eta_1 \sum_j \gamma_j \exp(i\mathbf{k}_1^j\mathbf{r}) \tag{17}$$

The energy of the atomic distribution described by (17) is

$$E = \frac{1}{2} N \left[V(0)c^2 + V(\mathbf{k}_o)(c\eta)^2 + V(\mathbf{k}_1)(c\eta)^2 \sum_j |\gamma_j|^2 \right] \tag{18}$$

This representation is correct for an arbitrary interaction potential, W(**r**), so long as the wave vectors $\mathbf{k}_0$ and $\{\mathbf{k}_1^j\}$ minimize the functions V(**k**) and $\tilde{V}(\mathbf{k})$, respectively. The thermodynamics of the sequence of ordering reactions is then determined by only three energy parameters: V(0), $V(\mathbf{k}_0)$ and $V(\mathbf{k}_1)$. The other V(**k**) do not appear because the associated amplitudes, $|\tilde{n}(\mathbf{k})|^2$, vanish in the macroscopic distribution.

The sequence of ordering reactions is not necessarily terminated by secondary ordering. If the composition of the resulting ordered phase deviates from stoichiometry then the third law requires that further ordering or decomposition occur until only stoichiometric phases appear.

IV. The Effective Oxygen-Oxygen Interaction

As in refs. [1,2,15] we consider structural changes in $YBa_2Cu_3O_{6+\delta}$ that involve only the reconfiguration of oxygen atoms on the oxygen interstitial sublattice of basal sites in the three-layer perovskite unit cell (Fig. 1). The associated change in the configurational part of the free energy is governed by the effective interaction of oxygen atoms on the interstitial sublattice, which we take to be a two-body interaction. A crucial test for the form of the two-body interaction is its ability to provide the correct ground state structure for the orthorhombic (O) phase of $YBa_2Cu_3O_7$. To enforce the observed crystallographic registry of the oxygen atoms on successive (001) planes of the three-layer perovskite structure of the O-phase the O-O interaction should have an effective range that at least exceeds the distance c = 3a between neighboring (001) basal planes, where a is the edge length of the elementary perovskite cell. This requires that the oxygen-oxygen interaction remain significant to at least the 15th coordination shell.

The same conclusion is reached from analysis of bonding in oxides in general [24], and $YBa_2Cu_3O_{6+\delta}$ in particular, which, like all perovskites, is expected to include a large coulombic contribution. In the specific case of $YBa_2Cu_3O_{6+\delta}$, Baetzold [21], Whangbo et al. [22] and Valkalahti and Welch [23] have all shown that the atomic positions in the basic lattice can be calculated to very high accuracy (within 0.03 Å for the major bond lengths [21]) by assuming that the interaction is the sum of a coulombic long-range interaction supplemented by a short-range core repulsion and a Van der Waals attraction.

These considerations lead to the conclusion that the O-O configurational interaction is long-range and largely coulombic. The coulomb interaction is screened by free carriers in $YBa_2Cu_3O_{6+\delta}$, and is certainly supplemented by short-range terms. The simplest realistic form is, hence,

$$W(\mathbf{r}) = \frac{(z^*)^2}{r} \exp\left(-\frac{r}{r_D}\right) + \delta W(\mathbf{r}) \tag{19}$$

where **r** is the vector separation between oxygen ions on the basal sublattice, r is its magnitude, r_D is the Debye screening radius, and $z^* = \frac{z}{\sqrt{\varepsilon}}$ is the effective charge of the oxygen

ion, where z is the ionic charge and ε is the dielectric constant. The dielectric constant (ε) accounts for the effects of electron shell polarization and displacements of the ions.

The screening radius, r_D, cannot be too large since the density of holes in $YBa_2Cu_3O_{6+\delta}$ is sufficient to provide significant screening. On the other hand, the radius, r_D, cannot be too small since the interaction potential must ensure registry between the oxygen arrangements on adjacent (001) basal planes that are separated by three perovskite unit cells. We hence consider an intermediate case, and take $r_D = 8a_1 \approx 5.7a$, where $a_1 = a/\sqrt{2}$ is the nearest-neighbor distance between O atoms, when a numerical value is needed.

A perturbation, $\delta W(\mathbf{r})$, to the screened coulomb interaction in (19) is dictated by the fact that the screened coulomb potential oversimplifies the oxygen-oxygen interaction at small separation distances. The potential neglects the spatial dispersion of the dielectric constant, which may be substantial at distances of the order of the crystal lattice parameter. It also neglects short-range interactions, which include contact repulsion from overlap of the electron shells and short-range attraction by van der Waals forces. The contact repulsion only affects close neighbors, and should have only a small effect on the short-range O-O interaction since the oxygen ions are never nearest neighbors. The van der Waals attraction decreases sharply with the separation distance, but will contribute to the interaction of near neighbors on the basal sublattice.

We also assume that the corrections, $\delta W(\mathbf{r})$, depend only on the separation distance $\mathbf{r}$. There is a subtlety in this assumption. When the positions of the host atoms are taken into account in Fig. 1 the interstitial oxygen positions in the basal plane are crystallographically equivalent, but are not related by lattice translations. The corner and base-centered sites on the interstitial sublattice have immediate environments that differ by a rotation of $\pi/2$. If the oxygen-oxygen interaction does not include the multi-particle interactions involving the host atoms the distinction between the two types of sites does not matter. However, in the real case the replacement of an oxygen atom by a vacancy will introduce a local strain or electronic polarization whose crystallographic orientation depends on the site type. This effect can be included in the model, but is usually ignored in the structural analysis of oxides on the grounds that the site-independent coulomb interaction is much stronger. In the present case, including the site distinction substantially complicates the mathematics of the model without improving the physics in any obvious way, so we have ignored it.

V. Identification of the Preferred Ordered Structures

(100) Order: The O Phase

The Fourier transform, $V(\mathbf{k})$, of the screened coulomb potential (the first term in equation (19)) has its minimum value at $\mathbf{k}_0 = \frac{2\pi}{a}(100)$, which is associated with the Lifshitz point at the mid-point of the (200) fundamental reciprocal lattice vector of the interstitial sublattice shown on Fig. 1. Since the extremum arises from symmetry its position is independent of the potential; specific investigation shows that it remains the least minimum

when the screened coulomb potential is perturbed by short-range functions $\delta W(r)$, so long as the total potential decreases monotonically.

With the minimum of V(k) at $k_o = \frac{2\pi}{a}(100)$, the structure of the primary ordered phase is described by the atomic distribution (eq. (15))

$$n_o(\mathbf{r}) = c + c\eta_o \cos(\mathbf{k}_o\mathbf{r}) = c + c\eta_o \cos(2\pi x) \tag{20}$$

The interstitial lattice sites, **r**, are at vector positions, **r** = (ax, ay, 3az), where a is the perovskite lattice parameter and x, y, z are the coordinates of the interstitial site. In the completely ordered state $n_o(\mathbf{r})$ assumes two values, 1 and 0, $c = c_{st} = \frac{1}{2}$ and $\eta_o = 1$. Hence, $\delta_{st} = 2c_{st} = 1$, giving the chemical formula $YBa_2Cu_3O_7$, which is the stoichiometric formula for the 123 compound. The atomic structure can be readily obtained by substituting the values of (x, y, z) at the interstitial sites (x and y are the doublets of integers and half-integers whose sum is an integer, z is an integer) into equation (20) and placing oxygen atoms at those sites where $n_o(x,y,z) = 1$. This procedure generates the superstructure whose unit cell is shown in Fig. 2.

If the Y, Ba, Cu, and O atoms of the host lattice are inscribed into the unit cell shown in Fig. 2, the structure is that of orthorhombic-123 phase. Therefore, the primary ordering caused by the screened coulomb interaction produces a tetragonal-orthorhombic phase transition (T→O) on cooling that leads to the high-T_c orthorhombic phase of $YBa_2Cu_3O_{6+\delta}$.

If a nonstoichiometric O phase is cooled then the system must decompose or order further; the thermodynamic preference is governed by the position of the minimum of the function $\tilde{V}(\mathbf{k})$ defined in eq. (16). A numerical analysis of the function $\tilde{V}(\mathbf{k})$ in the first Brillouin zone for a screened coulomb potentials with screening radii, $r_D > 3a_o$, leads to the conclusion that there are only two minima, at $\mathbf{k}_1 = \frac{2\pi}{a}(\frac{1}{2}00)$ and at $\mathbf{k}_1' = \frac{2\pi}{a}(\frac{11}{22}0)$. Variations of the screening radius, r_D, as well as short range corrections to the screened coulomb potential (19) do not change the positions of the minima if they do not affect the sign and monotonic decrease of the interaction potential. However, they do change the relative values of $\tilde{V}(\mathbf{k}_1)$ and $\tilde{V}(\mathbf{k}_1')$. The fact that the function $\tilde{V}(\mathbf{k})$ has only two minima at $\mathbf{k} \neq 0$ for a monotonic repulsive potential leads to two important general conclusions: (i) the secondary phase transition is certainly a secondary ordering, and (ii) only the two secondary ordered phases related to the $\{\frac{1}{2}00\}$ and $\{\frac{11}{22}0\}$ superlattice points, respectively, are possible. Which of these is the more stable is determined by the relative values of $\tilde{V}(\mathbf{k}_1)$ and $\tilde{V}(\mathbf{k}_1')$.

$(\frac{1}{2}00)$ Secondary Order: The O' Phase

The star of the vector $\mathbf{k}_1$ in the primary ordered phase contains two vectors, $\{\mathbf{k}_1\} = \pm\mathbf{k}_1 = \pm\frac{2\pi}{a}(\frac{1}{2}00)$. The secondary ordered phase generated by the star, $\{\frac{1}{2}00\}$, contains the superlattice point (100) inherited from the primary ordered phase and superlattice points at

$(\frac{1}{2}00)$ and $(\frac{\bar{1}}{2}00)$ that are associated with the secondary order. The atomic distribution for this case is, from eq. (17),

$$n_1(\mathbf{r}) = c + c\eta_o \cos(\mathbf{k}_o\mathbf{r}) + \eta_1 c\,[\gamma \exp(i\mathbf{k}_1 \mathbf{r}) + \gamma^* \exp(-i\mathbf{k}_1\mathbf{r})]$$

$$= c + c\eta_o \cos(2\pi x) + \eta_1 c\,[\gamma \exp(i\pi x) + \gamma^* \exp(-i\pi x)] \qquad (21)$$

The stability criterion for an ordered phases [27-29] requires that the number of distinct values taken by the atomic distribution function, $n(\mathbf{r})$, on the lattice sites be greater by one than the number of stars that generate the structure (which is equal to the number of different lro parameters). In the specific case of the distribution (21) the number of different lro parameters is 2 (η_o and η_1). This means that the coefficients γ should be chosen so that the function (21) has only three distinct values at crystal lattice sites. This is possible only if γ is a real number. Defining $\gamma = 1$ (this can always can be done by redefining the lro parameter, η_1), we have:

$$n_1(\mathbf{r}) = n_1(x,y,z) = c + c\eta_o \cos(2\pi x) + 2c\eta_1 \cos(\pi x) \qquad (22)$$

The function $n_1(\mathbf{r})$ describes the $(\frac{1}{2}00)$ phase. It has distinct values on three different sets of interstitial sites:

$$n_1^{(1)} = c + c\eta_o + 2c\eta_1,\ n_1^{(2)} = c + c\eta_o - 2c\eta_1,\ n_1^{(3)} = c - c\eta_o \qquad (23)$$

In the completely ordered state $n_1(\mathbf{r})$ must have the value 1 or 0 at every lattice site. This occurs, consistent with eq. (23), when $c = c_{st} = \frac{1}{4}$ and $\eta_o = \eta_1 = 1$; then $n_1^{(1)} = 1$, and $n_1^{(2)} = n_1^{(3)} = 0$. Since $\delta = 2c_{st} = \frac{1}{2}$, the stoichiometric formula of the $(\frac{1}{2}00)$ ordered phase is $YBa_2Cu_3O_{6.5}$. The atomic arrangement can be obtained by placing oxygen atoms on those interstitial sites for which $n_1(x,y,z) = n_1^{(1)} = 1$ and leaving vacant positions where $n_1(x,y,z) = n_1^{(2)} = n_1^{(3)} = 0$. The resulting structure is drawn in Fig.3 where positions of the O and Cu atoms in a (001) Cu-O basal plane are indicated. The positions of atoms in all other basal planes are identical since the function $n_1(x,y,z)$ does not depend on z. It is clear from Fig.3 that the structure is orthorhombic.

The energy of the $(\frac{1}{2}00)$ phase can be computed directly from eq. (7). Recognizing that the only concentration waves that have non-zero amplitudes are those associated with the wave vectors $\mathbf{k} = 0$, $\mathbf{k}_o$, $\mathbf{k}_1$ and $-\mathbf{k}_1$, and that the amplitudes of these are, respectively, c, $c\eta_o$, $c\eta_1$ and $c\eta_1$, the energy is

$$E = \frac{Nc^2}{2}[V(0) + V(\mathbf{k}_o)\eta_o^2 + 2V(\mathbf{k}_1)\eta_1^2] \qquad (24)$$

Note that while the interatomic interaction has an arbitrarily long range the energy of the $(\frac{1}{2}00)$ phase depends only on the three parameters V(0), $V(\mathbf{k}_o)$ and $V(\mathbf{k}_1)$ which are combinations of an arbitrary number of values of the potential, $W(\mathbf{r})$, at the sites of the interstitial sublattice.

$(\frac{11}{22}0)$ Order

The star of the wave vector $\mathbf{k}_{1'} = \frac{2\pi}{a}(\frac{11}{22}0)$ contains the two vectors $\mathbf{k}_{1'}^{(1)} = \frac{2\pi}{a}(\frac{11}{22}0)$ and $\mathbf{k}_{1'}^{(2)} = \frac{2\pi}{a}(\frac{\bar{1}1}{22}0)$. The secondary ordered phase generated by the star, $\{\frac{11}{22}0\}$, contains the superlattice point of the primary ordered phase, (100), along with superlattice points $(\frac{11}{22}0)$ and $(\frac{\bar{1}1}{22}0)$ that are introduced by the secondary order. The atom distribution in the $(\frac{11}{22}0)$ phase is, from eq. (17),

$$n_{1'}(\mathbf{r}) = n_{1'}(x,y,z) = c + c\eta_o \cos(\mathbf{k}_o\mathbf{r}) + \eta_1[\gamma_1 \exp(i\mathbf{k}_{1'}^{(1)}\mathbf{r}) + \gamma_2 \exp(i\mathbf{k}_{1'}^{(2)}\mathbf{r})]$$

$$= c + c\eta_o \cos(2\pi x) + \eta_1 c\{\gamma_1 \exp[i\pi(x+y)] + \gamma_2 \exp[i\pi(x-y)]\} \tag{25}$$

By the stability criterion the function $n_{1'}(\mathbf{r})$ can take no more than three independent values on the interstitial sites since there are only two lro parameters. This is true only if $\gamma_1 = \gamma_2 = \gamma$. Setting $\gamma = 1$, we have

$$n_{1'}(\mathbf{r}) = n_{1'}(x,y,z)$$

$$= c + c\eta_0 \cos(2\pi x) + \eta_1 c\{\exp[i\pi(x+y)] + \exp[i\pi(x-y)]\} \tag{26}$$

The function (26) describes the atomic distribution in the $(\frac{11}{22}0)$ secondary ordered phase. It assumes one of three values on the interstitial sublattice sites; these are the same as the values given by equation (23) for the $(\frac{1}{2}00)$ phase. Also like the $(\frac{1}{2}00)$ phase, the $(\frac{11}{22}0)$ phase is stoichiometric when $c = \frac{1}{4}$ and $\eta_o = \eta_1 = 1$, in which case it has the formula, $YBa_2Cu_3O_{6.5}$. The oxygen order in the basal plane of the $(\frac{11}{22}0)$ phase is shown in Fig. 4. Since $n_{1'}(\mathbf{r})$ does not depends on z, the structure is the same in all basal planes. The structure has a "2a×2a" pattern. It follows from Fig. 4 that it is orthorhombic.

The energy of the $(\frac{11}{22}0)$ phase can be found as in eq. (7), and is:

$$E = \frac{Nc^2}{2}[V(0) + V(\mathbf{k}_0)\eta_0^2 + 2V(\mathbf{k}_{1'})\eta_1^2] \tag{27}$$

Note that the energy expressions (24) and (27) for the enthalpy of the $(\frac{1}{2}00)$ and $(\frac{11}{22}0)$ phases are identical in form; they differ only in the value of the energy parameter in the third term, which is $V(\mathbf{k}_1)$ for the $(\frac{1}{2}00)$ phase and $V(\mathbf{k}_{1'})$ for the $(\frac{11}{22}0)$ phase. Since the distributions (22) and (26) of the two phases generate the same occupation numbers the entropies of the two secondary ordered phases are also the same:

$$S = -k_B \sum_{\mathbf{r}} \{ n_1(\mathbf{r}) \ln[n_1(\mathbf{r})] + [1 - n_1(\mathbf{r})] \ln[1 - n_1(\mathbf{r})] \}$$

$$= -\frac{Nk_B}{4} \sum_{j=1}^{3} \left\{ n_1^{(j)} \ln[n_1^{(j)}] + [1-n_1^{(j)} \ln[1-n_1^{(j)}] \right\} \tag{28}$$

where the occupation probabilities, $n_1^{(j)}$, (j = 1,2,3) are given by equations (23). It follows that the free energies of the two phases have the same functional form. For the $(\frac{1}{2}00)$ phase,

$$F = \frac{Nc^2}{2}[V(0) + V(\mathbf{k}_o)\eta_0^2 + 2V(\mathbf{k}_1)\eta_1^2]$$

$$+ \frac{Nk_BT}{4} \sum_{j=1}^{3} \left\{ n_1^{(j)} \ln[n_1^{(j)}] + [1-n_1^{(j)} \ln[1-n_1^{(j)}] \right\} \tag{29}$$

while for the $(\frac{11}{22}0)$ phase the parameter $V(\mathbf{k}_1)$ is replaced by $V(\mathbf{k}_{1'})$. The free energy difference is simply proportional to the difference in these parameters. Hence, *the $(\frac{1}{2}00)$ secondary ordered phase is more stable if $V(\mathbf{k}_1) < V(\mathbf{k}_{1'})$. and vice versa.*

Relative Stability of the $(\frac{1}{2}\,0\,0)$ and $(\frac{11}{22}\,0)$ phases

Direct calculation shows that when the potential is the simple screened coulomb potential

($\delta W(\mathbf{r}) = 0$ in eq. (19)) then $V(\mathbf{k}_1) > V(\mathbf{k}_{1'})$; specifically, with $r_D = 8a_1$, $V(\mathbf{k}_1) = -0.68\frac{(z^*)^2}{a_1}$, while $V(\mathbf{k}_{1'}) = -1.022\,\frac{(z^*)^2}{a_1}$.

Hence the $(\frac{11}{22}0)$ phase is preferred. However, this conclusion is not decisive. A small short-range deviation from the coulomb interaction, which is expected here, may reverse the relative magnitudes of $V(\mathbf{k}_1)$ and $V(\mathbf{k}_{1'})$ and stabilize the $(\frac{1}{2}00)$ phase. For example, Fig.7 shows an O-O potential, $W(\mathbf{r})$, in which the screened coulomb potential is supplemented by a short-range contribution, $\delta W(\mathbf{r})$, which affects only interactions with the nearest and next nearest neighbors. Although the short-range contribution is small (~ 0.1 of $W_0(\mathbf{r})$ for the affected coordination shells), the potential, $W(\mathbf{r}) = W_0(\mathbf{r}) + \delta W(\mathbf{r})$, stabilizes the $(\frac{1}{2}00)$ phase. The reason is that a two-neighbor interaction has a very different effect on the energies of the two secondary ordered phases. It does not change the energy of the $(\frac{1}{2}00)$ phase but significantly affects the $(\frac{11}{22}0)$ phase.

To show this we note that the contribution of $\delta W(\mathbf{r})$ to the Fourier transform of the potential $V(\mathbf{k})$ is

$$\delta V(\mathbf{k}) = \sum_{\mathbf{r}} \delta W(\mathbf{r}) e^{-i\mathbf{kr}}$$

$$= 4\delta W_1 \cos(\pi h)\cos(\pi k) + 2\delta W_2[\cos(2\pi h)+\cos(2\pi k)]$$

$$+ 4\delta W_3 \cos(2\pi h)\cos(2\pi k)$$

$$+ 4\delta W_4[\cos(3\pi h)\cos(\pi k)+\cos(\pi h)\cos(3\pi k)] + \ldots \qquad (30)$$

where the indices (hkl) are the coordinates of a reciprocal lattice point that is associated with the wave vector $\mathbf{k} = \frac{2\pi}{a}(hkl)$. Substituting the indices (100), $(\frac{1}{2}00)$ and $(\frac{11}{22}0)$, respectively, into eq. (30) yields the result

$$\delta V(\mathbf{k}_0) = -4\delta W_1 + 4\delta W_2 + 4\delta W_3 + \ldots \qquad (31a)$$

$$\delta V(\mathbf{k}_1) = -4\delta W_3 + \ldots \qquad (31b)$$

$$\delta V(\mathbf{k}_{1'}) = -4\delta W_2 + 4\delta W_3 + \ldots \qquad (31c)$$

It follows from eq. (31b) that a perturbation, $\delta W(\mathbf{r})$, that is confined to the first two coordination shells does not affect the potential $V(\mathbf{k}_1)$ and thus does not affect the thermodynamics of the $(\frac{1}{2}00)$ phase. On the other hand, the perturbation adds the potential $\delta V(\mathbf{k}_{1'}) = -4\delta W_2$ to the potential $V(\mathbf{k}_{1'})$, and hence changes the relative stability of the $(\frac{11}{22}0)$ phase. If δW_2 is negative (the net short-range correction is attractive in the second neighbor shell) then the energy of the $(\frac{11}{22}0)$ phase is raised relative to that of $(\frac{1}{2}00)$, and the $(\frac{1}{2}00)$ phase may become stable.

This result suggests that a close competition between the $(\frac{1}{2}00)$ and $(\frac{11}{22}0)$ phases may be resolved by short-range interaction terms. This perspective is supported by recent experimental observations. Electron microdiffraction studies [31,16,17] of samples with stoichiometries below $\delta = 0.5$ have revealed an ordered phase called the "2a x 2a" which actually is the $(\frac{11}{22}0)$ phase described above. The "$2\sqrt{2}$a x $2\sqrt{2}$a" phase reported in [31,16,17] is also derivatives of the $(\frac{11}{22}0)$ phase; it can be formed from the $(\frac{11}{22}0)$ phase through tertiary ordering. These observations suggest that small perturbations in the O-O interaction may shift the delicate thermodynamic balance between the $(\frac{11}{22}0)$ and $(\frac{1}{2}00)$ phases in favor of the former. The shift may particularly occur due to increases in the screening radius at stoichiometries below $\delta = 0.5$ (which stabilizes the $(\frac{11}{22}0)$ phase) caused by a reduction of the hole concentration in this composition range.

According to equations (31), the $(\frac{1}{2}00)$ phase is preferred if the screened coulomb potential is supplemented by a two-neighbor potential, $\delta W(\mathbf{r})$, whose value in the second coordination shell, δW_2, is sufficient to raise $V(\mathbf{k}_{1'})$ above $V(\mathbf{k}_1)$. From the values given above this requires

$$\delta W_2 \leq -0.0835\left[\frac{z^2}{\varepsilon a_1}\right] \tag{32}$$

The perturbation at the first neighbor shell, δW_1, it does not affect the stability of the $(\frac{1}{2}00)$ phase with respect to $(\frac{11}{22}0)$, but does alter stability with respect to the (100) phase.

VI. The Phase Diagram

The Quantitative Model

We began this investigation to study possible forms of the phase diagram of $YBa_2Cu_3O_{6+\delta}$ if the O' $(\frac{1}{2}00)$ phase is stable. In the context of the model this can only happen if the screened coulomb potential is supplemented by a short-range interaction whose value at the second coordination shell satisfies the constraint, $\delta W_2 \leq -0.0835\left[\frac{z^2}{\varepsilon a_1}\right]$. The free energy describing the equilibrium between the T, O and O' phases is then given by equation (25). The free energy function (25) depends on $W(\mathbf{r})$ only implicitly through the Fourier transforms $V(0)$, $V(\mathbf{k}_0)$ and $V(\mathbf{k}_1)$. When the interaction is primarily electrostatic the Fourier transform $V(0)$ at the origin of the $\mathbf{k}$-space vanishes due to the electroneutrality condition:

$$V(0) = 0 \tag{33}$$

so that only the two parameters $V(\mathbf{k}_0)$ and $V(\mathbf{k}_1)$ appear. There are two ways to fix the numerical values of these parameters to calculate the phase diagram: (1) define $W(\mathbf{r})$ numerically by setting the values of the parameters r_D, ε, δW_1 and δW_2 and take the appropriate Fourier transforms, or (2) find the values $V(\mathbf{k}_0)$ and $V(\mathbf{k}_1)$ directly by fitting experimental results. We shall take the latter approach since it involves fewer assumptions. However, while $W(\mathbf{r})$ uniquely determines $V(\mathbf{k}_0)$ and $V(\mathbf{k}_1)$, the converse is not true; the exact values of δW_1 and δW_2 are not fixed by $V(\mathbf{k}_0)$ and $V(\mathbf{k}_1)$. Many different potentials, $W(\mathbf{r})$, determine the same phase diagram.

To find the phase diagram we first rewrite equation (25) in the dimensionless form:

$$\tilde{F} = \frac{F}{|V(\mathbf{k}_0)|} = \frac{1}{2}N\Big\{-(c\eta_o)^2 + 2\zeta(c\eta_1)^2$$

$$- \frac{\tau}{4}\Big[(c+c\eta_o+2c\eta_1)\ln[c + c\eta_o +2c\eta_1) + (1-c-c\eta_o-2c\eta_1)\ln(1-c-c\eta_o-2c\eta_1)$$

$$+ (c+c\eta_o-2c\eta_1)\ln(c+c\eta_o-2c\eta_1) + (1-c-c\eta_o -2c\eta_1)\ln(1-c-c\eta_o-2c\eta_1)$$

$$+ 2\left((c-c\eta_0)\ln(c-c\eta_0) + (1-c+c\eta_0)\ln(1-c+c\eta_0)\right)\Big]\Big\} \tag{34}$$

where $\zeta = V(\mathbf{k}_1)/|V(\mathbf{k}_0)|$ is a dimensionless interaction parameter, $\tau = k_BT/|V(\mathbf{k}_0)|$ is a dimensionless temperature, and we have used the fact that $V(\mathbf{k}_0)$ is negative. The minimization of the free energy (34) with respect to the long range order parameters, η_0 and η_1, yields two equations for the equilibrium values of these parameters,

$$\frac{\partial \tilde{F}}{\partial \eta_0} = \frac{\partial \tilde{F}}{\partial \eta_1} = 0 \tag{35}$$

These equations have bifurcation points at the order-disorder temperatures for the primary $T \rightarrow O$ and secondary $O \rightarrow O'$ $(\frac{1}{2}00)$ phase ordering, which are both second-order transitions in the present model. The bifurcation temperatures are given by the equations

$$\tau_1^o = \frac{T_1^o}{|V(\mathbf{k}_0)|} = c(1-c) \tag{36a}$$

$$\tau_2^o = \frac{k_BT_2^o}{|V(\mathbf{k}_0)|} = -(c + c\eta_0^e)(1 - c - c\eta_0^e)\zeta \tag{36b}$$

where η_0^e is the equilibrium value of the lro parameter at $\tau = \tau_1^0$, which is determined by the first of equations (36), T_1^o is the temperature of the $T \rightleftharpoons O$ primary ordering, T_2^o is the temperature of the $O \rightleftharpoons O'$ secondary ordering in a system with fixed composition, c. Taking the first partial derivative of (35) shows that η_0^e has the form

$$\ln\left[\frac{(c+c\eta_0^e)(1-c+c\eta_0^e)}{(c-c\eta_0^e)(1-c-c\eta_0^e)}\right] = -\frac{2c\eta_0^e}{\tau_2^0} \tag{37}$$

The transcendental equations (36b) and (37) can be solved simultaneously for τ_2^0, the value of the reduced temperature at which the O phase spontaneously orders into $O'(\frac{1}{2}00)$, as a function of the ratio, ζ, and the composition $c = 2\delta$.

According to ref. [19] the temperature, T_1^0, of the $T \rightleftharpoons O$ primary ordering at $\delta = 0.5$ $(c = \frac{1}{4})$ is 973 K. Using these values in eq.(36a) yields

$$V(\mathbf{k}_0) = -5190k_B \tag{38}$$

According to ref. [16,32], when $YBa_2Cu_3O_7$ is reduced isothermally ($\frac{1}{2}$00) diffraction spots appear if the temperature is below ~ 400°C, but are not observed at higher temperatures. This suggests that the maximum temperature for congruent O ⇌ O' ordering (at δ = 0.5) is near 400°C. Assuming this value, T_2^0 = 400°C = 673 K at c = 0.25. Then, with $V(\mathbf{k}_0) = -5190k_B$, $\tau_2^o = k_B T_2^0/|V(\mathbf{k}_o)| = 0.13$. The solution of equations (36b) and (37) for the two variables, ζ and η_o^e at $\tau_2^o = 0.13$ gives $\eta_o^e \approx 0.87$ and $\zeta = -0.52$. Since $V(\mathbf{k}_1) = \zeta V(\mathbf{k}_0)$ and $V(\mathbf{k}_0) = -5190k_B$,

$$V(\mathbf{k}_1) = -2700k_B \tag{39}$$

in units of degrees K.

Physical Plausibility of the Quantitative Model

Before exhibiting the phase diagram that is determined by the values of the interaction parameters given in (38) and (39) we investigate whether these lead to a self-consistent model with a physically plausible interaction potential, W(r). Specifically, the inferred values of $V(\mathbf{k}_0)$ and $V(\mathbf{k}_1)$ should yield a reasonable value of the dielectric constant and a small, attractive short-range interaction that stabilizes the ($\frac{1}{2}$00) ordered phase.

First, we compute the dielectric constant. Since the Fourier transform, $V(\mathbf{k}_1)$, does not depend on the short-range corrections, it can be calculated from the screened coulomb potential. For $r_D = 8a_1$, direct computation of the Fourier transform, $V(\mathbf{k})$, at the point $\mathbf{k}_1 = \frac{2\pi}{a}(\frac{1}{2}00)$ gives

$$V(\mathbf{k}_1) = -0.688\,\frac{z^2}{\varepsilon a_1} \tag{40}$$

Substituting this result into equation (39) with $a_1 = a/\sqrt{2} = 2.71\times 10^{-8}$ cm and z = 2e, where e is the electron charge, yields an estimate for the dielectric constant:

$$\varepsilon \approx 90 \tag{41}$$

This is a physically reasonable value for an oxide in the perovskite structure.

Next we find the quantitative perturbation of the primary ordering parameter, $V(\mathbf{k}_0)$, by the short-range interaction. The coulomb contribution to $V(\mathbf{k}_0)$ is

$$V(\mathbf{k}_0)_{cb} = \left[\frac{z^2}{\varepsilon a_1}\right]\sum_{\mathbf{r}}\left(\frac{a_1}{r}\right)\exp\left(-\frac{r}{r_D}\right)\exp(-i\mathbf{k}_0\cdot\mathbf{r})$$

$$= -1.494\left[\frac{z^2}{\varepsilon a_1}\right] = -5850k_B \tag{42}$$

in degrees K, where we have used eq. (41). The parameter $V(\mathbf{k}_0)$ is the sum of the contributions of the coulomb and the short-range interactions. Using equations (38), (42) and (31a), the short-range perturbation is

$$\delta V(\mathbf{k}_0) = V(\mathbf{k}_0) - V(\mathbf{k}_0)_{cb} \approx -4\delta W_1 + 4\delta W_2 = 660k_B \tag{43}$$

Hence the short-range perturbation is a small (~10%) correction to the energy parameter $V(\mathbf{k}_0)$; as assumed, the coulomb interaction gives the major contribution to the oxygen-oxygen interaction.

The third test test for the self consistency of the model is the requirement that $(\frac{1}{2}00)$ order be preferred to $(\frac{11}{22}0)$. This requirement is met if the inequality (32) holds; with $\frac{z^2}{\varepsilon a_1} = 3920k_B$ we must have $\delta W_2 < -327k_B$, in which case $\delta W_1 > -492k_B$ from eq. (42). Hence the O' phase is preferred for secondary ordering when

$$\delta W_1 > -0.126\frac{z^2}{\varepsilon a_1} = -492k_B$$

$$\delta W_2 < -0.0835\frac{z^2}{\varepsilon a_1} = -327k_B \tag{44}$$

The chosen values of $V(\mathbf{k}_0)$ and $V(\mathbf{k}_1)$ do not fix the values of δW_1 and δW_2 beyond these inequalities; however, the assumption that δW_1 and δW_2 are small and attractive is consistent. A specific example of a suitable potential, $W(\mathbf{r})$, is presented in Fig. 5; the short-range perturbations are $\delta W_1 = -0.1255\frac{z^2}{\varepsilon a_1}$ and $\delta W_2 = -0.0855\frac{z^2}{\varepsilon a_1}$. The Fourier transforms $V(\mathbf{k})$ and $\tilde{V}(\mathbf{k})$ determined by this potential are drawn in Figs. 6 and 7. The minimum value of the Fourier transform, $V(\mathbf{k})$, falls at $\mathbf{k}_0 = \frac{2\pi}{a}(100)$. Hence, like the pure screened coulomb potential, this potential establishes a thermodynamic preference for the orthorhombic primary ordered 123 phase whose atomic distribution is described by eq. (18) and shown in Fig.2. The potential $\tilde{V}(\mathbf{k})$ (Fig.7) has two minima. However, the minimum at $\mathbf{k}_1 = \frac{2\pi}{a}(\frac{1}{2}00)$ is slightly deeper than that at $\mathbf{k}_{1'} = \frac{2\pi}{a}(\frac{11}{22}0)$; the $(\frac{1}{2}00)$ phase is more stable at govern concentration, and, thus, provides the preferred secondary ordering of the orthorhombic O-phase.

The equilibrium phase diagram is determined by the free energy function (34). Given the inferred values of $V(\mathbf{k}_0)$ and $V(\mathbf{k}_1)$ (eq. (38) and (39)), the dimensionless parameter ζ has the value, - 0.52. The phase diagram calculated for $\zeta = -0.52$ is shown in Fig.8. This diagram includes a T + O two-phase field below approximately 860 K, with a peritectoid reaction to an equilibrium O' phase $(\frac{1}{2}00)$ near 470 K. Below this temperature two two-phase fields appear, T + O' and O + O'.

According to this phase diagram, the O' phase is only at equilibrium for a narrow range of stoichiometry at temperatures below 470 K (≈ 200°C). However, the O' phase can appear above this temperature as a metastable phase. Since ordering requires atomic migration over a microscopic length ~ 1Å while decomposition requires diffusion over at least a nanoscale length, ordering occurs much faster than decomposition. Therefore, in

many cases the observed transformations of the system will be governed by metastable congruent ordering. The congruent ordering diagram calculated with the energy parameters (38), (39) is shown in Fig.9. Congruent ordering from a metastable O phase to metastable O' occurs at temperatures well above the peritectoid line over a broad composition range. Figs. 10a and 10b show the calculated values of the long-range order parameters, η_0 and η_1, respectively, plotted against the background of the congruent ordering diagram.

VII. Discussion

The calculated phase diagram that is plotted in Fig. 8 has a second-order transition line between the tetragonal (disordered) T phase and the orthorhombic (ordered) O phase. This line terminates at a tricritical point at ~ 860 K, where it bifurcates into two solvus lines that envelope a two-phase T + O field. The two-phase field lies above a horizontal peritectoid line at ~ 470 K. Below the peritectoid line the phase diagram includes two two-phase fields on either side of an intervening $(\frac{1}{2}00)$ O' phase region. These are O + O' and O' + T fields.

The diagram is calculated on the assumption that the oxygen-oxygen interaction is a screened coulomb interaction beyond the second-nearest distance between oxygen atoms. The potential deviates from this form for the nearest and next nearest interactions only. This approximation is a conventional one that is commonly used in calculations of oxide structures (see, for example, the reviews in ref. [24]) that has produced results in very good agreement with the structures, elastic moduli and dielectric constants of oxides. Similar potentials have been applied to the $YBa_2Cu_3O_7$ oxide by Baeltzold [21], Whangbo et al. [22] and Bekker et al. [23]. The calculated structures are in very good agreement with the structural data. For example, Baeltzold reports agreement in bond lengths within ~ 0.03Å.

The calculated phase diagram is almost independent of the details of short-range perturbation, $\delta W(\mathbf{r})$. It is determined by two fitting parameters, $V(\mathbf{k}_0)$ and $V(\mathbf{k}_1)$, as long as the values of the short-range perturbations, $\delta W(\mathbf{r})$, are within the O' phase stability range given by the inequality (44). The importance of the short-range perturbation is to stabilize the $(\frac{1}{2}00)$ O' phase against the alternative $(\frac{11}{22}0)$ ordered phase.

The fitting parameters, $V(\mathbf{k}_0)$ and $V(\mathbf{k}_1)$, are chosen by matching the computed phase relationships at two points: the T $\rightleftharpoons$ O and O $\rightleftharpoons$ O' second order transition temperatures at c = 0.25 (δ = 0.5). The first of these temperatures is reasonably well accepted. The second is inferred from transmission electron microscopic studies by Amelinckx, Van Tandeloo and coworkers [16,32]; it is imprecise and subject to refinement. However, the computed diagram predicts a transformation behavior of $YBa_2Cu_3O_{6+\delta}$ that agrees with expectation and experiment in several encouraging respects.

First, the real-space interaction function, W(r), has the form expected for an oxide with the perovskite structure. The oxygen-oxygen interaction is primarily coulombic, and, given the fitted value of $V(\mathbf{k}_1)$, predicts a dielectric constant, $\varepsilon \approx 90$, which is a reasonable value for an oxide of the perovskite type. The short-range interaction is relatively small.

While its specific form is not uniquely determined, the first- and second-neighbor potentials are bounded by inequalities (44) which show that they can consistently be chosen to be small and attractive.

Second, the computed phase diagram predicts a peritectoid decomposition, O' ⇌ T+O at ≈190 °C, that agrees with the x-ray observations of Sood et al. [10] and Radhakrishnan et al. [11]. These researches observed the decomposition of orthorhombic $YBa_2Cu_3O_{6.73}$ and $YBa_2Cu_3O_{6.78}$ samples, respectively, into a mixture of T and O phases at 200 °C. This temperature is above the peritectoid temperature in the calculated diagram; thus the chosen compositions are inside the T + O field of the stable diagram. In ref. [11] the stoichiometries of the coexisting T and O phases were estimated to be near 6.15 and 6.92, respectively, from the position of the x-ray lines. These values were also consistent with the volume fractions of the T and O phases which were measured independently. The values found for the equilibrium concentrations of the coexisting T and O phases at 200 °C agree very closely with the computed phase diagram.

Third, the computed phase diagram is consistent with experimental observations [17,18] that suggest a very narrow equilibrium field for the O' phase, while the computed congruent transformation diagram is consistent with observations by the same workers that the O' phase appears in samples with a wide range of stoichiometries. The calculated equilibrium and congruent diagrams also suggest that there is no real contradiction between experimental reports of O and O' coexistence at compositions between $YBa_2Cu_3O_{6.5}$ and $YBa_2Cu_3O_{6.8}$ [9] and other reports [10,11] of T and O phase coexistence in the same composition range. The superficial contradiction is resolved if the samples, which were observed at room temperature, are assumed to be in "quenched" equilibrium states related to different high-temperature two-phase fields. The O and O' phases coexist at temperatures below the peritectoid temperature, ≈190 °C, while the T and O phases coexist at higher T. These interpretations are especially plausible in light of the slow kinetics of decomposition in this system. According to ref. [11] the aging time required for decomposition at 200 °C is very long, 672h for $YBa_2Cu_3O_{6.78}$. Thus, the decomposition is difficult to observe. The congruent ordering that results in the formation of the O' phase does not require long-range diffusion, so this reaction should be much faster and much easier to observe, in agreement with the experience of many investigators.

Fourth, the model is consistent with the occasional appearance of $(\frac{11}{22}0)$ order, exhibited in the "2a x 2a" phase and the closely related "$2\sqrt{2}$a x $2\sqrt{2}$a phase" [16-18,31]. The screened coulomb potential provides a minimum for the $(\frac{11}{22}0)$ secondary ordering wave that is very close to that for $(\frac{1}{2}00)$ ordering. A suitable minor perturbation of the system would cause the appearance of metastable phases with this type of order.

Fifth, the calculated congruent transformation diagram provides a simple explanation for the drop in the superconducting transition temperature, T_c, from ≈90 K to ≈60 K when the overall composition drops below $\delta \approx 0.8$. It follows from the position of the congruent ordering line in Fig. 9 that the O → O' transformation near room temperature starts at $\delta < 0.8$. If a sample is cooled quickly enough to suppress decomposition (which appears

to be the case in most experiments) the O-phase order is lost by secondary decomposition when $\delta < 0.8$.

Tertiary ordering of the O' phase may also occur in quenched samples to create superstructures derivative of the $(\frac{1}{2}00)$ phase whose natural stoichiometry matches the current stoichiometry of the material. The theory of such ordering in $YBa_2Cu_3O_{6+\delta}$ was developed previously by the present authors [15] by extending the theory of the homologous series of Magneli phases in ceramic materials that have long-range repulsive interactions between ordering atoms (such as Ti_nO_{2n-1} and Mo_nO_{3n-1}) [33,34]. According to [15] a homologous series of Magneli structures should be found with the generic formula, $YBa_2Cu_3O_{7-\frac{n}{2n+1}}$, where n is an integer. In the Magneli phases the excess oxygen atoms form interstitial planar defects in the $(\frac{1}{2}00)$ phase that are periodically repeated. If the diffusion rate is insufficient to provide the ordering of the interstitial planar defects that forms the Magneli phases, a random, disordered distribution of these defects should appear. It has been shown that these defects provides a broadening of the $(\frac{1}{2}00)$ diffraction spots if the number of the defects is small (small deviation from the stoichiometry ($\delta = 0.5$) and results in the shift of the diffraction maximum from the $(\frac{1}{2}00)$ position if the deviation from ideal stoichiometry is larger [35].

The agreement of these predictions with electron diffraction observations by Zhu et al.[36] and Beyers et al.[18] seems to confirm this picture of the nonstoichiometric structure of the undercooled O' phase. The prediction that remains to be tested experimentally is that within the O' area on the congruent diagram shown in Fig.9 the nonstoichiometric O' phase is inherently inhomogeneous due to formation of a macroscopically large number of planar interstitial (100) defects, which may be periodic or not, depending on the kinetics. From oxygen balance considerations the fraction of the defects is given by the ratio $\frac{2\delta-1}{1-\delta}$ [35]. This inhomogeneity in the internal state should have important consequences for the properties of material in the stoichiometry range $0.5 < \delta < 0.8$, including both the superconducting transition and the magnetic properties.

If we consider only the T and O phases the diagram given in Fig. [8] has one of the two forms predicted by the authors in ref. [1]. It differs from the computed diagram proposed in ref. [2] in two respects: the inclusion of the O' equilibrium field at low temperature and the absence of a miscibility gap in the O-phase field. The latter difference results from a small change in the values of the interaction parameters.

Acknowledgement

The authors are grateful for support from the Director, Office of Energy Research, Office of Basic Energy Sciences, U.S. Department of Energy, under Contract No. DE-*AC03-76SF00098* (J.W.M.).and from the National Science Foundation under grant No.*NSF-DMR-88-17922*,(A.G.K)

References

1. A.G. Khachaturyan, J.W. Morris, Jr., Phys. Rev. Lett. **59**, 2776 (1987).

2. A.G. Khachaturyan, S.V. Semenovskaya, and J.W. Morris, Jr., Phys. Rev. B37, 2243 (1988).

3. M. Sarikaya and E. Stern, Phys. Rev., **B37**, 9373 (1988).

4. C.M. Chen,.J. Werder, L.F. Schneemeyer, P. Gallagher, and J.V. Waszczak, Phys. Rev., **B38**, 2888 (1988).

5. D.J. Werder, C.M. Chen, R.J. Cava, and B. Batlogg, Phys. Rev., **B38**, 5130 (1988).

6. Z. Hiroi, M. Takano, Y. Ikeda, Y. Takeda, Y,. Bando, Jpn. Journ. of Appl. Phys., **27**, L141 (1988).

7. B. Raveau, C. Michel, M. Hervieu, and J. Provost,Physica C 153-155, 3 (1988).

8. Y. Xu, M. Suenaga, J. Tafto, R.L. Sabatini, A.R. Moodenbaugh and P. Zolliker (to be published).

9. M. You, J.D. Axe, X.B. Kan, S. Hashimoto, S.C. Moss, J.Z. Liu, G.W. Crabtree, and D.J. Lam, Phys. Rev., **B38**, 9213 (1988).

10. A.K. Sood, K. Sankarah, V.S. Sastry, M.P. Jayaawadhar, C.S. Sundar, J. Janaki, S. Vijayalakshami, and Y. Harihazahan, Physica **C 156**, 720 (1988).

11. T.S. Radhakrishnan, J. Janaki, G.V.N. Rao, S. Kalavathy, V.S. Sastry, Y. Hariharan, M.P. Janawadkar, K. Govinda Rajan, P. Parameswaran, and O.M. Sreedharan (to be published in Pramana- Journ. of Physics, India).

12. G. Burns, F.M. Dacol, F. Holtzberg, and D.L. Kaisen, Solid State Commun., **66**, 217, (1988).

13. G. Van Tandeloo, H.W. Zanderbergen and S. Amelinckx, Solid State Comm., **63**, 289, 606 (1987).

14. R.M. Fleming, L.F. Schneemyer, P.K. Gallagher, B. Batlogg, L.W. Rupp, and J.V. Waszczak, Phys. Rev., **B37**, 7922 (1988).

15. A.G. Khachaturyan and J.W. Morris, Jr., Phys. Rev. Letter, **61**, 215, (1988)

16. S. Amelinckx, G. Van Tandeloo, J. Van Landuyt, in Proc. of the Stanford International on Materials and Mechanisms of Superconductivity in High Temperature Superconductors, July 23-28,1989, Stanford, CA

17. J. Reyes-Gasga, T. Krekels, G. Van Tandeloo, J. Van Landuyt, S. Amelinckx, W.H.M. Bruggink and H. Verweij , Physica **C 159**, 831, (1989)

18. R.Beyers, B.T. Ahn, G. GormanV.Y. Lee, S.S.P. Parkin, M.L. Ramirez, K.P. Roche, and J.E. Vazques, T.M. Gur and R.A. Huggins (to be published in Nature)

19. J.D.Jorgensen, M.A.Beno, D.G.Hinks, L.Soderholm, H.J.Volin, R.L.Hitterman, J.D.Grace, I.K. Schuller, C,V, Serge, K.Zhang and M.S. Kleefish, Phys. Rev. **B36**, 3608, (1987)

20. L.T. Wille, A. Berera, and D. de Fontaine, Phys. Rev. Letters, **60**, 1065, (1988); A.Berera and D.de Fontaine, Phys. Rev. **B 39**,6727 (1989)

21. R.C. Baetzold, Phys. Rev., **B 38**, 11304, (1988)

22. M.-H.Whangbo, M. Evain, M.A. Beno, U.Geiser, and J.M. Williams, Inorg. Chem., **27**, 467 (1988)

23. S.Valkealahty and D.O.Welch (Brookhaven National Laboratory, preprint BNL43072 (1989)

24. A.M. Stoneham, J.H. Harding, Annual Rev. Phys. Chem, 1986, 37, 53; Computer Simulation of Solids, Series Lecture Notes in Physics, vol. 166, ed. by C.R.A. Catlow and W.C. Mackrodt, Springe-Verlag, New York, 1982

25. V.G,Vaks, A.I. Larkin and S.A. Pikin, Sov. Phys. JETP **51**, 240 (1966)

26. R.A. Suris Sov. Phys. Solid State **4**, 850, (1962)

27. A.G.Khachaturyan, Phys. Met. Metallog. 13, 493 (1962) ; Sov. Phys. Solid State, **5**, 16, 548 (1963), "The Problems of Symmetry in Statistical Thermodynamics of Substitutional and Interstitial Ordered Solutions", (Review Article) Phys. Status Solidi (b)**60**,9, (1973)

28. A.G.Khachaturyan, "Ordering in Substitutional and Interstitional Solid Solutions", in Progress in Material Science, edited by J.W. Christian, P. Haasen and T. Massalski, Pergamon, Oxford, vol. **22**, 1/2 (1978)

29. A.G.Khachaturyan , Theory of Structural Transformations in Solids, Wiley and Sons, New York, 1983.

30. A.G.Khachaturyan, Kristallografia, **10**, 303, (1965);

31. C. Chaillout, M.A. Alario-Franco, J.J. Capponni, J. Chenavas, J.L. Hodeau, and M. Marezio, Phys. Rev. **B36**, 7118 (1987)

32. G. Van Tandeloo (private communication)

33. B.I. Pokrovskii and A.G. Khachaturyan, J. Solid State Chem., **61**, 154 (1986)

34. A.G. Khachaturyan and B.I.Pokrovskii, Concentration Wave Approach to Structural and Thermodynamic Characterization of Ceramic Crystals, in Progress in Material Science, edited by J.W. Christian, P. Haasen and T. Massalski, vol.**29**, pp.1-138 (1985), Pergamon Press, Oxford.

[35] A.G. Khachaturyan and J.W. Morris,Jr. " Diffuse Scattering by $YBa_2Cu_3O_{6+\delta}$ Oxides with Magneli-Type Interstitial Plane Defects " (accepted for publication in Phys. Rev. Letters, 1990)

36. Y.Zhu, A.R. Moodenbaugh, M. Suenaga and J. Tafto (Brookhaven National Laboratory, preprint 1989, to be published)

Figure Captions

Fig. 1 A unit cell of the sublattice of interstitial sites permitted for occupation by oxygen atoms within the range between $YBa_2Cu_3O_6$ - $YBa_2Cu_3O_7$. □ = interstitial sites.

Fig.2 A unit cell of the primary ordered phase described by equation (17). □ = interstitial sites, O = oxygen atoms. If host atoms, Y, Ba, Cu, and O are placed in their respective host lattice sites within this unit cell, the resultant atomic arrangement describes the unit cell of the orthorhombic $YBa_2Cu_3O_7$ phase.

Fig. 3 The positions of O atoms (empty circles) , oxygen vacancies (□), and Cu atoms (black circles) in the Cu-O (001) basal planes for the secondary ordered double-period $(\frac{1}{2}00)$ phase. The (x,y) coordinates of these atoms are the same at all (001) basal Cu-O planes.

Fig. 4 The positions of O atoms (empty circles), oxygen vacancies (□), and Cu atoms (black circles) in the Cu-O (001) basal planes for the secondary ordered, 2a×2a $(\frac{11}{22}0)$ phase. The (x,y) coordinates of these atoms are the same at all (001) basal Cu-O planes.

Fig. 5 An example of the dependence of the oxygen-oxygen interaction potential on the reduced separation distance, $\frac{r}{a_1}$. The solid line describes the screened coulomb potential with the screening radius, $r_D = 8a_1$. The points indicate the values of the potential, $W(\mathbf{r})$, slightly modified for the nearest and next-nearest separation distances to provide stability of the secondary ordered $(\frac{1}{2}00)$ phase over the secondary ordered $(\frac{11}{22}0)$ phase.

Fig. 6 The dependence of $V(\mathbf{k})$ on $\mathbf{k}$ for the modified oxygen-oxygen interaction potential presented in Fig. 5 along the $\mathbf{k} = \frac{2\pi}{a}$ (h00) and $\mathbf{k} = \frac{2\pi}{a}$ (hh0) directions in the first Brillouin zone of the interstitial sublattice shown in Fig. 1.

Fig. 7 The dependence of $\tilde{V}(\mathbf{k})$ on $\mathbf{k}$ for the modified oxygen-oxygen interaction presented in Fig. 5 along the $\mathbf{k} = \frac{2\pi}{a}$ (h00) and $\mathbf{k} = \frac{2\pi}{a}$ (hh0) directions in the first Brillouin zone of the primary ordered phase shown in Fig. 2.

Fig. 8 The calculated equilibrium phase diagram . T labels the stability field of the disordered tetragonal phase, O the stability field of the primary ordered orthorhombic 123 phase, O' the field of the double-period $(\frac{1}{2}00)$ phase. The diagram shows that the equilibrium O' phase is formed as a result of the peritectoid reactions T + O ⇌ O + O' or T + O ⇌ T + O' below ~ 190°C.

Fig. 9 The calculated congruent diagram describing T → O and O → O' congruent ordering. The solid lines indicate second-order transitions between T and O, and between O and O' phases.

Fig. 10 a. Thin lines indicate the equilibrium values of the lro parameter, η_0.
b. Thin lines indicate he equilibrium values of the lro parameter, η_1.
The dotted lines describe the conditional spinodal of the isostructural decomposition of the O and O' phases.

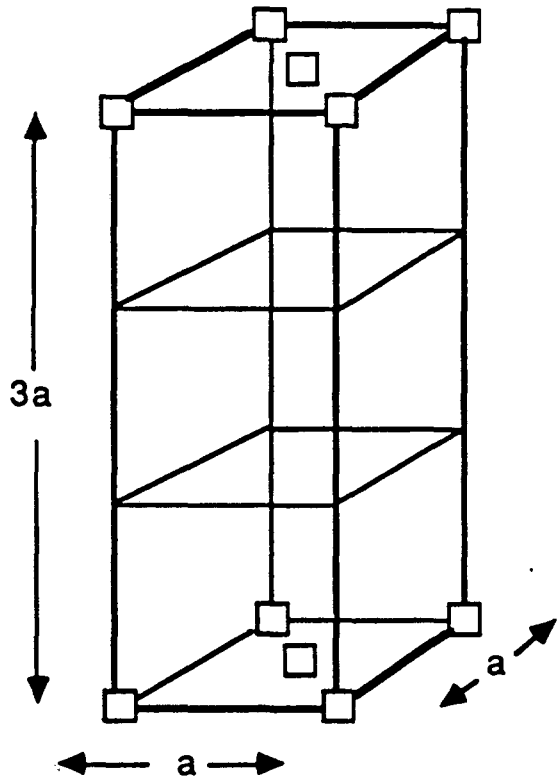

Figure 1

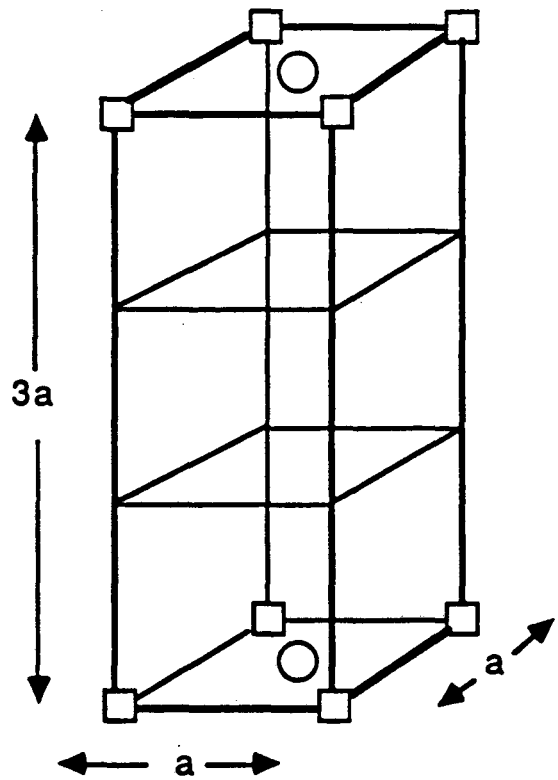

Figure 2

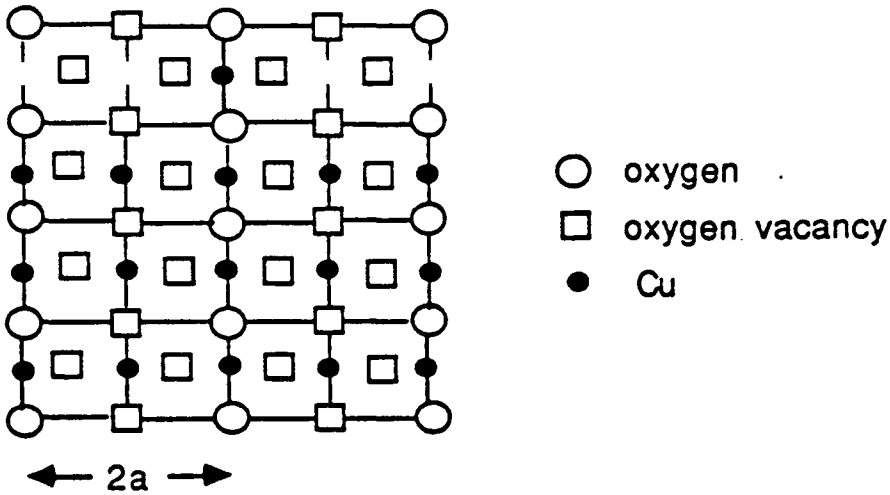

Figure 3

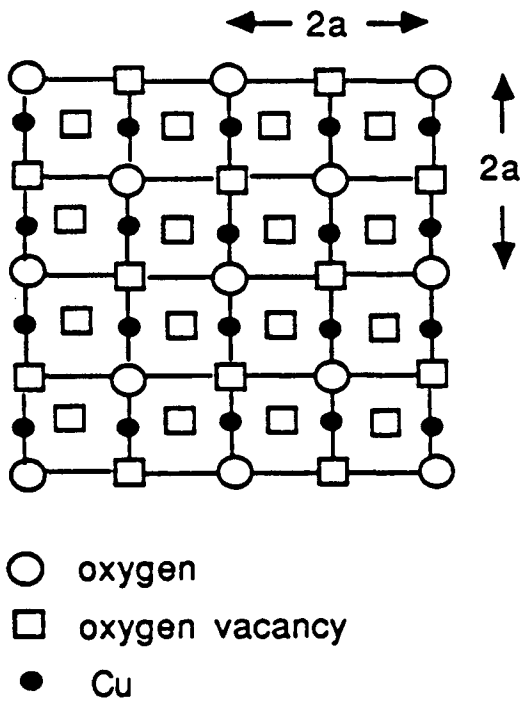

Figure 4

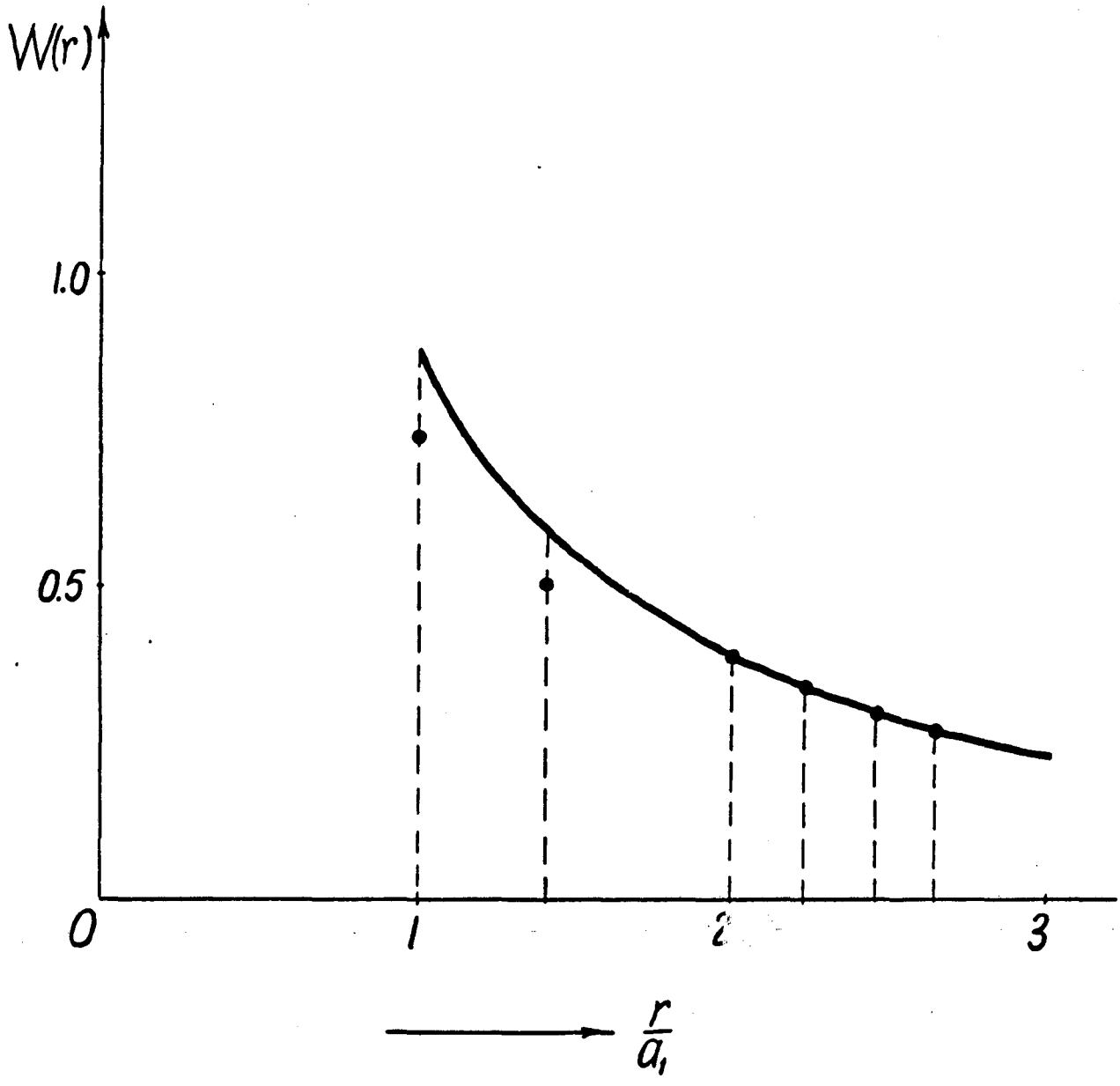

Figure 5

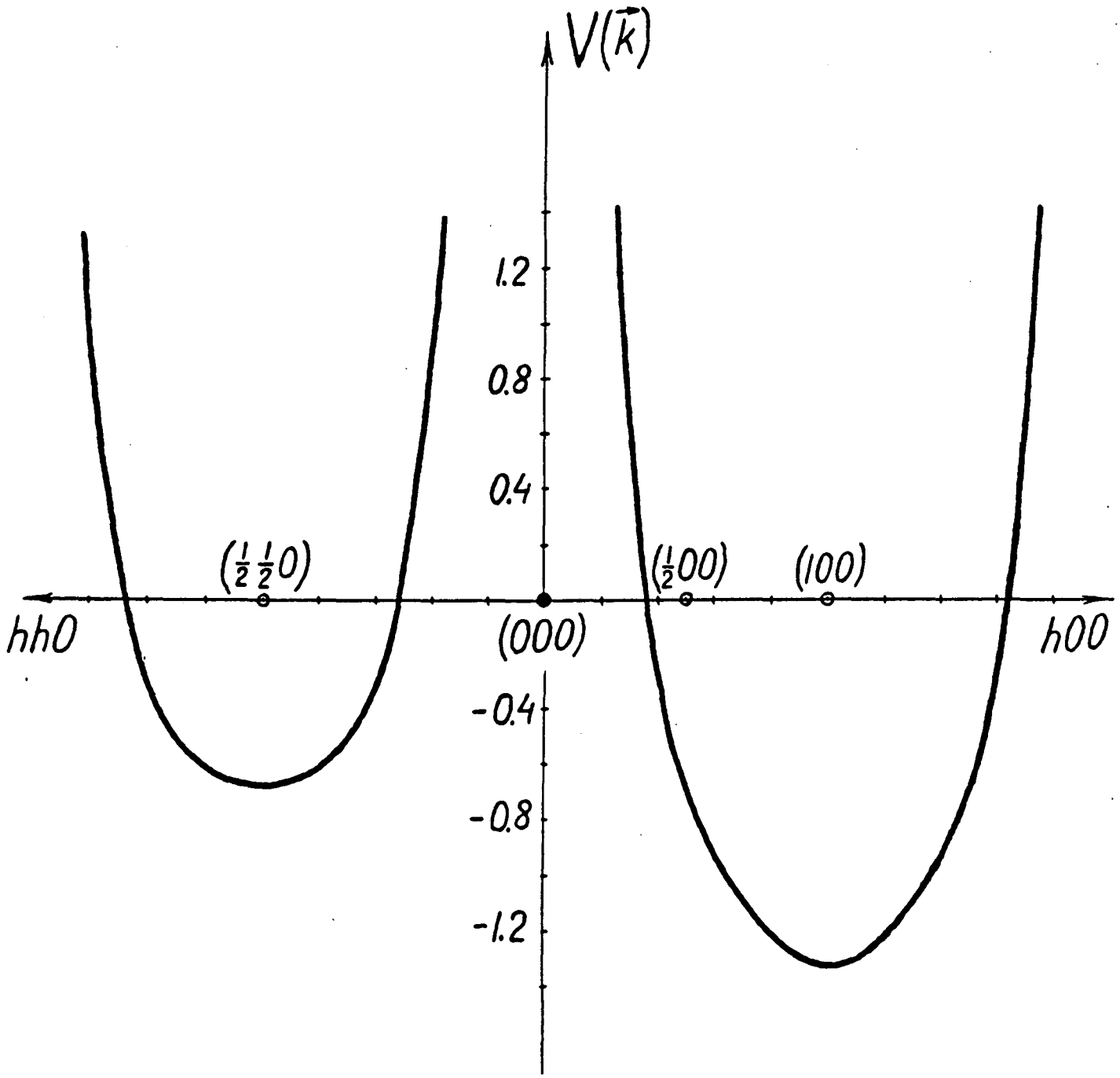

Figure 6

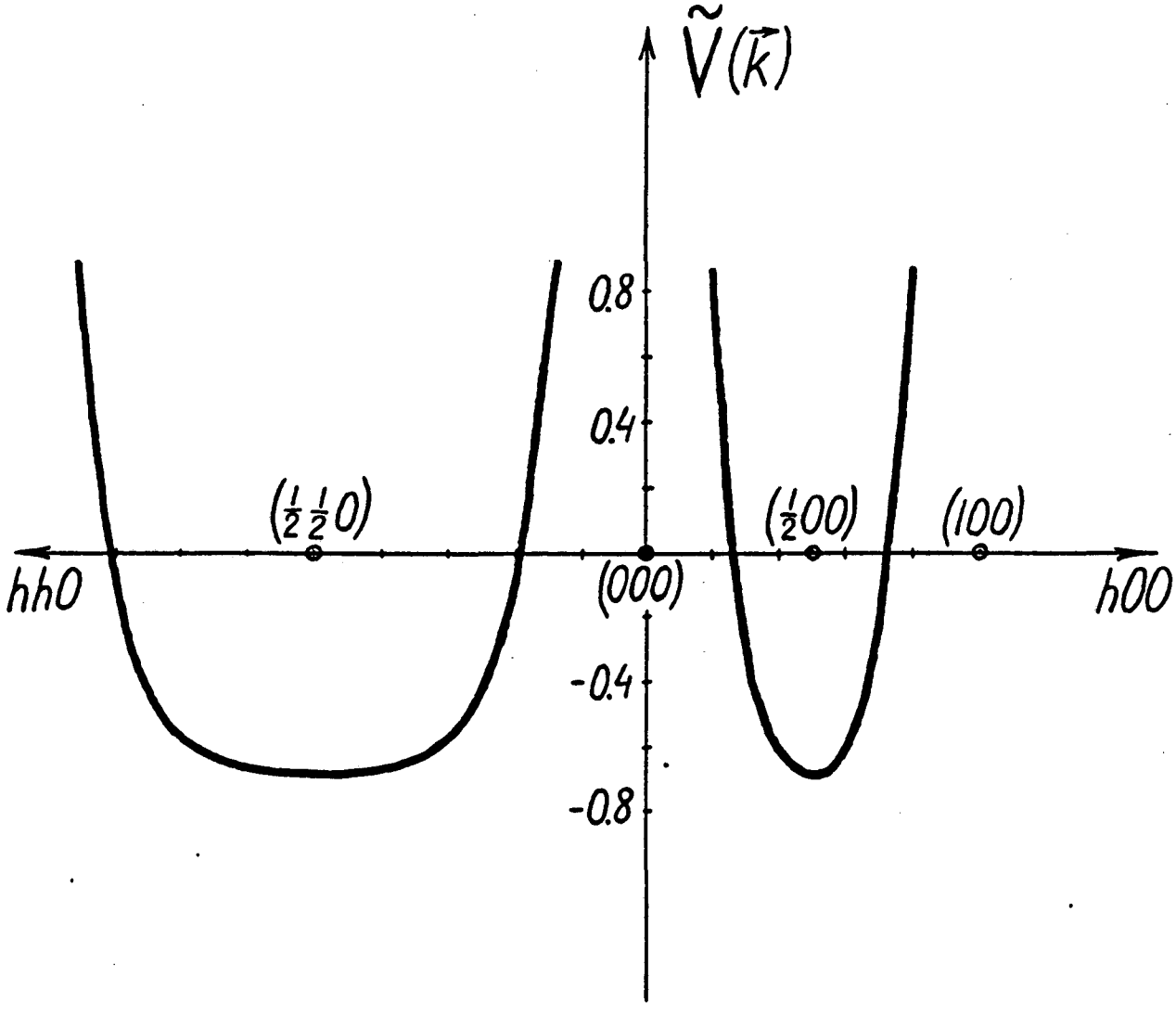
$\tilde{V}(\vec{k})$
0.8
0.4
-0.4
-0.8
$(\frac{1}{2}\frac{1}{2}0)$
$(\frac{1}{2}00)$
(100)
hh0
(000)
h00

Figure 7

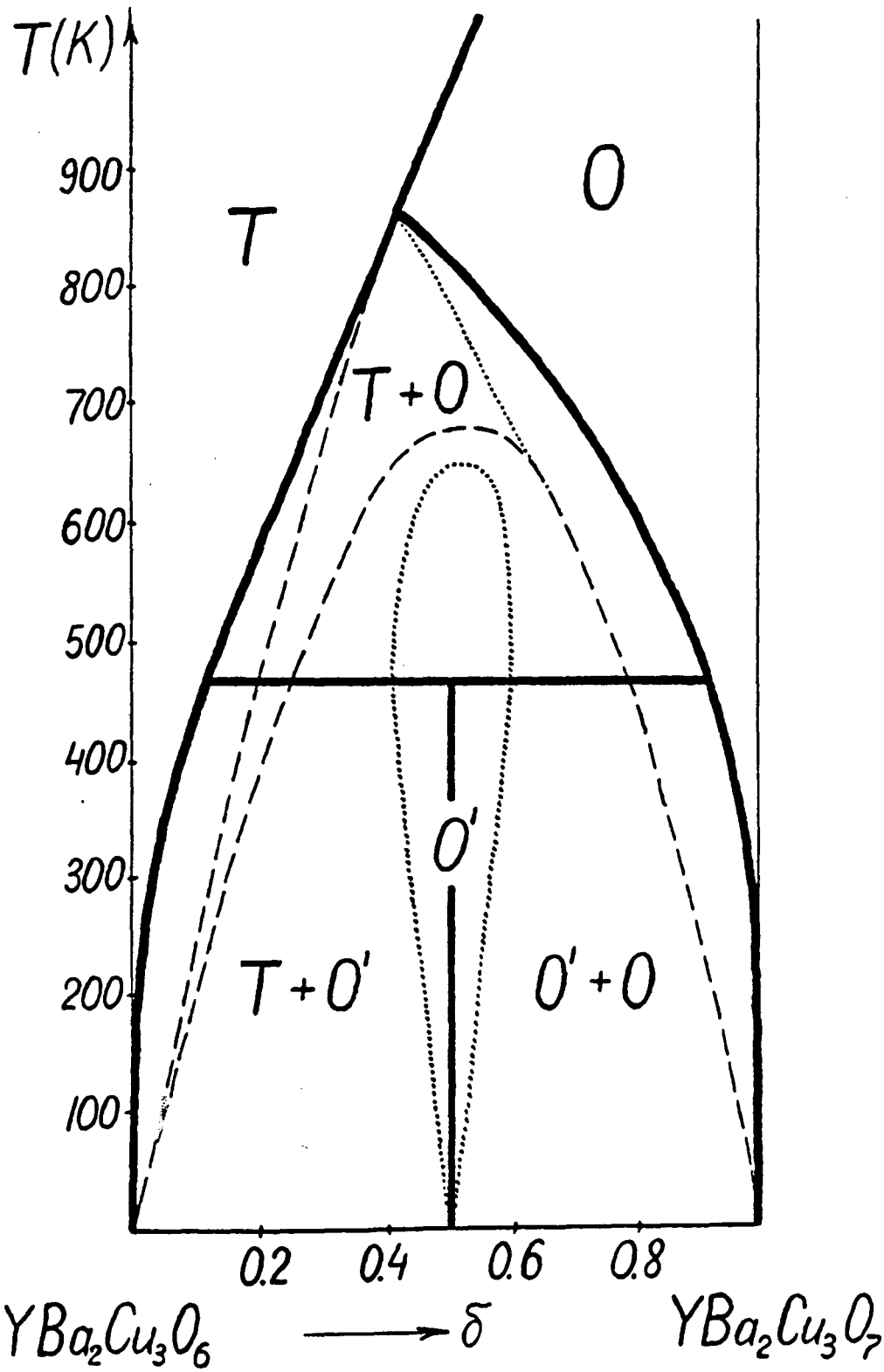
T(K)
900
800
700
600
500
400
300
200
100
T
O
T+O
O'
T+O'
O'+O
0.2
0.4
0.6
0.8
YBa2Cu3O6
δ
YBa2Cu3O7

Figure 8

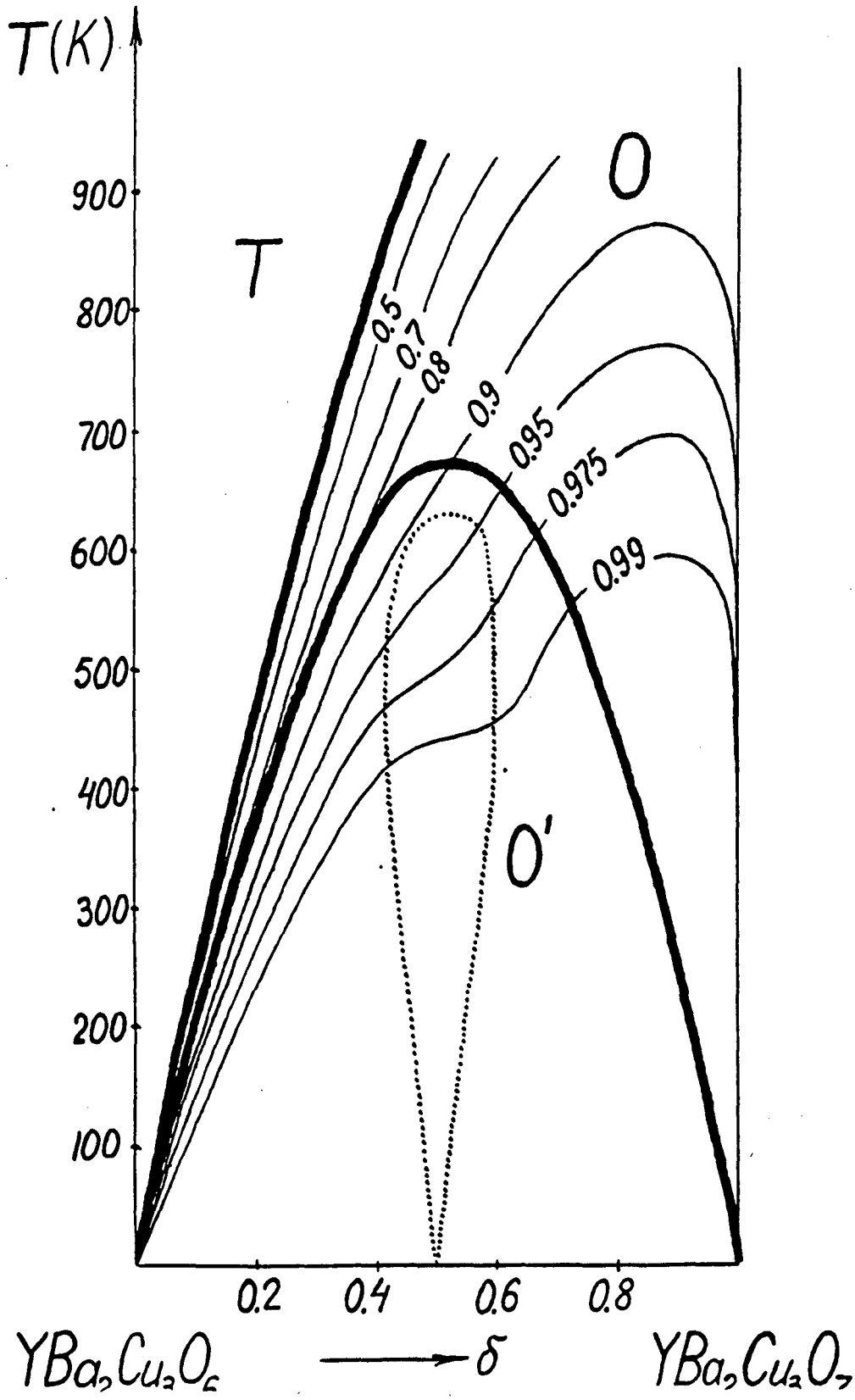
T(K)
900
800
700
600
500
400
300
200
100
T
O
O'
0.5
0.7
0.8
0.9
0.95
0.975
0.99
0.2
0.4
0.6
0.8
YBa2Cu2O6
δ
YBa2Cu2O7

Figure 9

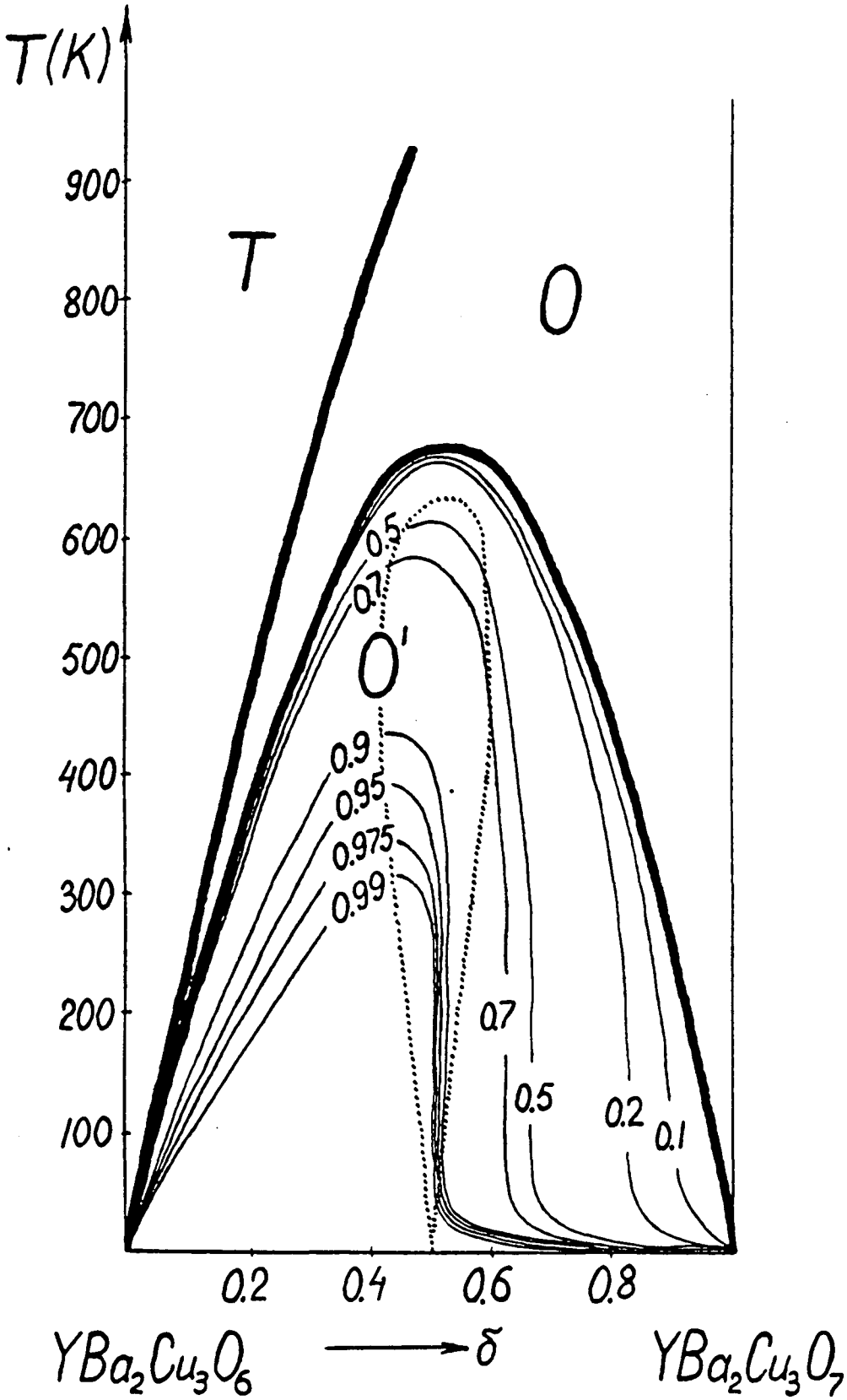
T(K)
900
800
700
600
500
400
300
200
100
T
O
O'
0.5
0.7
0.9
0.95
0.975
0.99
0.7
0.5
0.2
0.1
0.2
0.4
0.6
0.8
YBa2Cu3O6
δ
YBa2Cu3O7

Figure 10

LAWRENCE BERKELEY LABORATORY
CENTER FOR ADVANCED MATERIALS
1 CYCLOTRON ROAD
BERKELEY, CALIFORNIA 94720